From the Department of Dermatology, Allergology, and Venereology
of the University of Lübeck
Director: Prof. Dr. med. Detlef Zillikens

Genetics of Autoimmune Arthritis in the Mouse

Dissertation
for Fulfillment of Requirements
for the doctoral degree of the University of Lübeck

from the Department of Natural Sciences

Submitted by

Laura Mellado Ranea

from Chipiona, Spain

Lübeck 2012

First referee: Prof. Saleh Ibrahim

Second referee: Prof. Jürgen Rohwedel

Date of oral examination: 22 May 2013

Approved for printing. Lübeck, 24 May 2013

Contents

1 Introduction

1.1 Rheumatoid arthritis

1.1.1 General aspects of rheumatoid arthritis

Rheumatoid arthritis (RA) is a systemic chronic autoimmune inflammatory disease that primarily affects joints. RA can impair any synovial-lined diarthrodial joint and it mainly affects wrists and small joints of the hand. Although RA is considered an autoimmune disease, the autoantigen that triggers disease remains unknown. However, autoantibodies to citrullinated protein antigens (ACPA), also known as anti–cyclic citrullinated peptide (anti-CCP), and/or autoantibodies to the Fc portion of immunoglobulin G (IgG), called rheumatoid factor (RF), are present in 50-80% of RA patients [1] and can precede clinical manifestations by many years [2].

RA is characterized by cellular infiltration of the synovium and systemic inflammation. Synovial infiltrates consists primarily of fibroblast-like and macrophage-like synoviocytes, macrophages, several populations of T cells, and B cells. Joint inflammation can progress to cartilage erosion and bone destruction, leading to severe disability. Several inflammatory cascades can lead to this situation although the precise mechanisms of pathogenesis are still not completely understood. It is likely that RA is not a single disease but a heterogeneous group of overlapping syndromes. This assumption is supported by the fact that genetic and clinical differences are found between those RA patients who present autoimmunity to citrullinated protein antigens and those who do not. ACPA-positive patients have more aggressive clinical course and lower remission rates than ACPA-negative patients. In addition, both subsets of the disease have different genetic risk profiles [3].

Classification and Diagnosis

The American College of Rheumatology (ACR) and the European League Against Rheumatism (EULAR) have designed classification criteria for early and established RA

(Table 1.1) [4]. These new criteria differ from the former ACR 1987 criteria on the focus on features at earlier stages of disease that are associated with persistent and erosive disease, instead of defining the disease by its late-stage features.

Table 1.1. 2010 ACR/EULAR criteria

1. Joint involvement	(0–5)
• One medium-to-large joint	(0)
• Two to ten medium-to-large joints	(1)
• One to three small joints (large joints not counted)	(2)
• Four to ten small joints (large joints not counted)	(3)
• More than ten joints (at least one small joint)	(5)
2. Serology	(0–3)
• Negative RF and negative ACPA	(0)
• Low positive RF or low positive ACPA	(2)
• High positive RF or high positive ACPA	(3)
3. Acute-phase reactants	(0–1)
• Normal CRP and normal ESR	(0)
• Abnormal CRP or abnormal ESR	(1)
4. Duration of symptoms	(0–1)
• Less than 6 weeks	(0)
• 6 weeks or more	(1)

Scores are shown in parentheses. Patients with a score of ≥ 6/10 are classified as having RA. Additionally, patients may also be classified as having RA if they have typical erosions or long-standing disease previously satisfying the classification criteria [4]. RF, rheumatoid factor; ACPA, autoantibodies to citrullinated protein antigens; CRP, C-reactive protein; ESR, erythrocyte sedimentation rate.

Treatment

To date, there is no causative therapy to cure RA and most of the current treatments aim to mitigate symptoms. Analgesics and non-steroidal anti-inflammatory drugs (NSAIDs) are commonly used to reduce pain, and in addition, NSAIDs reduce stiffness and inflammation. However, these drugs do not affect disease progression [5, 6].

Over the last decade, the use of disease modifying antirheumatic drugs (DMARDs) has increased. These drugs reduce joint synovitis, systemic inflammation, disability and improve function; however, their diverse mechanisms of action are not fully understood [7]. The main DMARD is methotrexate but there are others such as sulfasalazine and leflunomide or Gold (rINN sodium aurothiomalate) and cyclosporin, though less used due to higher toxic effects. Hydroxychloroquine and chloroquine are used for their DMARD-like properties. DMARDs can be combined to improve efficacy [8]; however, their use is restricted as consequence of the adverse effects.

Glucocorticoids can be used in short terms to reduce joint inflammation and also in combination with DMARD [9]. Despite decreasing joint damage, long-term glucocorticoid therapy is limited due to the significant increase of adverse effects such as infections and osteoporosis [10].

The most recently developed drugs are the biological agents. TNF-inhibitor, Interleukin-6 inhibitor, B cell inhibitor and T cell costimulation inhibitor have been proven to be highly effective against RA. Nevertheless, caution and appropriate screening are needed to control secondary risk such as viral or bacterial infections [11].

There is an acute need to search for further therapies to increase response rates and to improve remission of the disease. Understanding of the basis of RA is a key step to achieve these objectives.

Epidemiology

RA affects between 0.5 - 1% of adult population in developed countries with a frequency three times higher in women than in men [12-14]. Prevalence increases with age, and is lower in developing countries [15]. RA incidence varies across populations, and ranges from 5 to 50 per 100,000 adults in developed countries [16, 17].

Environmental risk factors

Smoking is the most important risk factor and doubles the risk of developing RA. Smoking effect seems to be restricted to patients with ACPA-positive disease [18]. There are other potential environmental risk factors such as viral or bacterial infections, diet, oral contraceptive use or social stress; however, supporting evidences for these factors are weak [19].

1.1.2 Genetics of rheumatoid arthritis

Genetic factors have a strong impact in RA susceptibility and development [20]. The heritability of RA is estimated to be 60% [21]. The most important genetic risk is the human leukocyte antigen (HLA) locus. Its influence is estimated to be 30–50% to the overall genetic susceptibility to RA; however, it confers susceptibility only to ACPA-positive patients [22]. HLA-DRB1 shows the strongest association within the locus. The link between HLA-DRw4 and RA was found by Stastny et al. in the seventies in an association study [23]. Further studies showed the linkage with several alleles of the HLA-DRB1 locus which were later organized into the shared-epitope hypothesis [24]. The share epitope may influence peptide binding and contact between HLA-DR and T cell receptor, playing a role in the development of RA. In addition, recent studies describe the contribution of other HLA genes to RA susceptibility [25].

Other non-MHC regions have been associated with RA by genome-wide association studies (GWAS). *PTPN22*, *PADI4*, *STAT4* and TRAF1-C5 locus are generally accepted as associated with the disease, even though their role in RA pathogenesis has not been proven yet. After HLA-DRB1, the largest genetic factor for RA is *PTPN22* which was associated with ACPA-positive RA patients in a candidate-gene approach in 2004 [26]. The missense mutation in *PTPN22* affects T cell receptor signaling which supports its participation in the susceptibility of several autoimmune diseases as RA or systemic lupus erythematosus (SLE) (11).

A haplotype of *PADI4* has been strongly associated with susceptibility to RA in Asiatic population; however, its association in European populations is still controversial [27]. *PADI4* gene encodes one of the isoenzymes which catalyze the citrullination of arginine residues of proteins and may play a role in the production of ACPA [27].

The risk locus TRAF1-C5 has been linked to ACPA-positive RA patient [28]. *TRAF1* encodes a member of the TRAF family which acts as a negative regulator of signals by linking TNF [29]; *C5* encodes the component 5 of complement, which is implicated in inflammatory and cell killing processes. Both genes could be responsible of the increase of RA susceptibility.

With a more modest effect, *STAT4* has been associated to RA and SLE [30]. This gene encodes a transcription factor involved in IL-12 signaling in T cells and NK cells [31].

1.1.3 Mouse models of rheumatoid arthritis

Experimental models are extensively used to study the etiology and pathogenesis of complex diseases. Many animal models for RA have been developed, most probably each of them resembling a possible pathway which can lead to disease. Arthritis can arise in mice spontaneously or from induction, either by passive transfer of arthritogenic antibodies or by active immunization. Some spontaneous models include K/BxN TCR transgenic mice [32], TNF-α transgenic mice [33] and BXD2/TyJ mice [34]. Passive antibody transfer models, as anti-CII antibody-induced arthritis (ACIA) [35], are completely independent of the immune system. There are several active models as antigen-induced arthritis (AIA) [36], collagen-induced arthritis (CIA) [37], proteoglycan-induced arthritis (PGIA) [38] and glucose-6-phosphate isomerase (G6PI)-induced arthritis [39], each of one requiring different cell population from the adaptive and immune systems. In the present work, the models BXD2/TyJ and CIA have been used to investigate the genetic basis of arthritis.

BXD2/TyJ is a recombinant inbred strain generated by inbreeding for more than 20 generations a F2 progeny obtained by intercrossing C57BL/6J (B6) and DBA/2J [34].

BXD2/TyJ mice spontaneously develop chronic erosive arthritis and generalized autoimmune disease, including renal disease. Mice start to develop arthritis after 4 months with low incidence; however, between 9 and 12 months, 66% of females and 42% of males are affected. BXD2/TyJ mice produce high titers of antibodies against DNA and RF, with predominance of IgG1 and IgG2b isotypes. Adult mice are characterized by glomerulonephritis, proteinuria and splenomegaly [40]. BXD2/TyJ strain develops features of autoimmune diseases due to a complex combination of interacting genes inherited from the original parental strains, B6 and DBA/2J, which develop neither arthritis nor lupus. These characteristics make the BXD2/TyJ strain an exceptional model to study genetics of autoimmune diseases such as erosive arthritis.

CIA is one of the most widely used animal models for RA. Arthritis is elicited in mice by immunization with heterologous or autologous type II collagen (CII) emulsified in Freund´s adjuvant [37]. CIA resembles RA in several pathological features such as synovial hyperplasia, mononuclear cell infiltration, pannus formation, cartilage degradation and bone erosion. As in RA, the immunopathogenesis of CIA involves both T cell and B cell response, as it is proven by the resistance to disease of the respective knock out models [41, 42]. In contrast to BXD2/TyJ mice, no RF is present in CIA [43]. Susceptibility to disease is associated with certain MHC haplotypes, H-2r, H-2q and possibly H2-b. However, non-MHC genes play a role in the disease as it is demonstrated by the difference in the susceptibility to CIA between H-2q strains: DBA/1J strain (100%), B10q (84%), NFR/N (50%), B10g (41%), SWR/J (0%) and FVB/N (0%) [44, 45].

1.2 Identification of susceptibility genes in complex disease

The knowledge of genes and pathways involved in disease is of great importance to understand the pathogenic mechanisms of disease, and consequently to improve therapy, diagnosis and disease prevention. Linkage and association studies in human are commonly used to identify candidate susceptibility loci in Mendelian disorder; however, the heterogeneity of the human genome, the minor single gene contribution

to the pathogenesis and the multiplex gene-gene and gene-environment interactions make very challenging the identification of susceptibility genes in complex diseases, or quantitative traits. Quantitative traits are measurable phenotypic characteristics that vary over a range of distribution in a population and are influenced by genetic and/or environmental factors. The genetic locus controlling a quantitative trait is called quantitative trait locus (QTL). Frequently, quantitative traits are multifactorial and are affected by several polymorphic genes and environmental factors. In such cases, when more than one locus influence a given trait, the mapping and identification of all the causative QTLs become more difficult since each QTL which modulates the trait may have a different effect size (which will vary from strong to weak), may be influenced by the genetic background, and will probably interact with other QTLs.

Animal models are invaluable tools to decipher genetic factors affecting quantitative traits, since it is possible to control the genetic background and to define the environmental conditions. Inbred mouse strains are typically used for genetic studies. They are generated by long inbreeding and have a nearly identical genome. One of the advantages of mouse models is the availability of multiple strains with characteristic susceptibility to diseases and differences in their genome. Often, QTLs controlling a particular phenotype in mice and humans are situated in homologous regions [46]. Because the proportion of mouse genes with a counterpart in human (and vice versa) is 99% [47], once identified a susceptibility gene it is possible to confirm the association of the human homologous or its pathway with disease. In fact, it has been shown that the human homologous of genes underlying mouse QTLs were also controlling the corresponding human QTL [46].

Identifying the causal genes underlying QTLs is considered the next challenge in determining the genetic basis of complex diseases. To date, more than 4,100 QTLs have been published (according to the MGI database); however, few quantitative trait genes have been identified.

1.2.1 Strategies to identify and fine map QTLs

1.2.1.1 Identification of QTLs

There are different strategies to identify and refine QTLs [48]. The most traditional approach to locate disease loci in animal models is to cross two inbred strains with different traits for at least two generation (F2 intercross or N2 backcross) to produce heterozygous litters which carry recombinant genome from the parental strains and characteristic phenotypes. Then, by linkage analysis it is possible to identify and locate QTLs to a ~20 Mbp genome region [49].

1.2.1.2 Fine mapping

To increase the mapping resolution, it is required to narrow the confidential interval (CI) of, or to fine map, the indentified QTLs ideally to a ~1-2 Mbp region. Several approaches can be followed such as recombinant inbred strains, advance intercross line (AIL), heterogeneous stock (HS), congenics strains and *in silico* mapping [50].

Recombinant inbred strains. Recombinant inbred strains are developed by intercrossing two inbred strains to produce F1 offspring, followed by brother-sister intercrossing for at least 20 generations. Eventually, new inbred strains are produced, each of which is homozygous and carry unique loci combination of the original parental genomes [46].

Advanced intercross line (AIL). An AIL is produced by random and sequential intercrossing two or more inbred strains for many generations so that animals accumulate new recombinants. Unlike recombinant strains, brother–sister mating is avoided in AIL. This approach offers a high genomic resolution allowing to refine simultaneously multiples QTLs and to separate QTLs with different contributions which were originally comprised in a large QTL [51, 52]. AIL method has also been successfully applied to identify new QTLs [53].

Heterogeneous stock (HS). HSs are AIL originated from several founder strains (Figure 1.1). HSs are kept in heterozygosis by semi-random breeding. Currently, there are two 8-way advance intercross available [50].

In silico *mapping*. Comparative analysis of haplotype structures in the locus of interest from inbred strains that differ in the trait of interest might reveal blocks that segregate appropriately with the trait, and consequently, are candidate regions to contain the causative polymorphism [54].

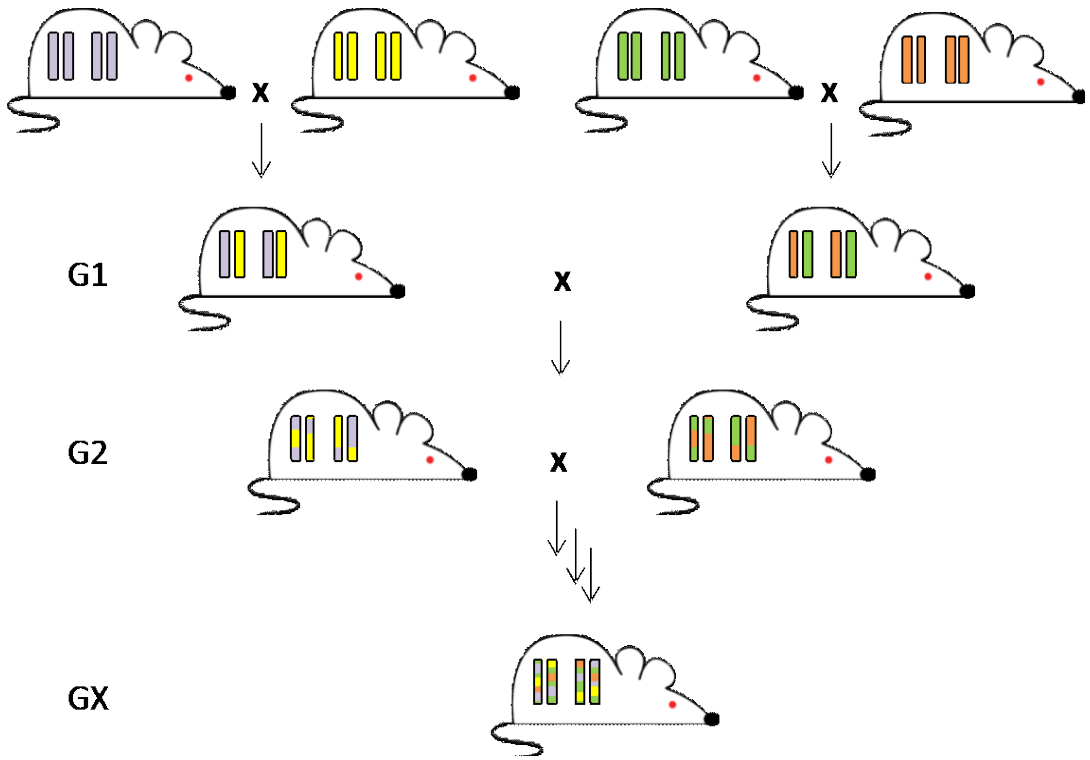

Figure 1.1. Heterogeneous stocks. High genomic resolution is obtained in HSs due to the accumulation of many recombination events. HSs are a powerful approach to identify and refine QTLs.

Congenic strains. Congenic strains are the mainstay of fine-mapping in mice. A congenic strain is a genetically modified inbred strain that contains a genomic locus from one

inbred strain (donor strain) and the remainder of its genome from the background or recipient strain. They are generated by repeated backcrosses of one strain into another during several generations, with appropriate selection of the region of interest [55] (Figure 1.2). The number of generations necessary to create a congenic strain can be reduced if a speed congenic approach is used. For that, also the presence of disturbing donor alleles outside of the desired locus is determined. When a single gene is isolated in a congenic strain, the trait can be analyzed as a Mendelian trait in the congenic strain compared to the wildtype strain. However, only genes with high penetrancy can be identified by this kind of positional cloning.

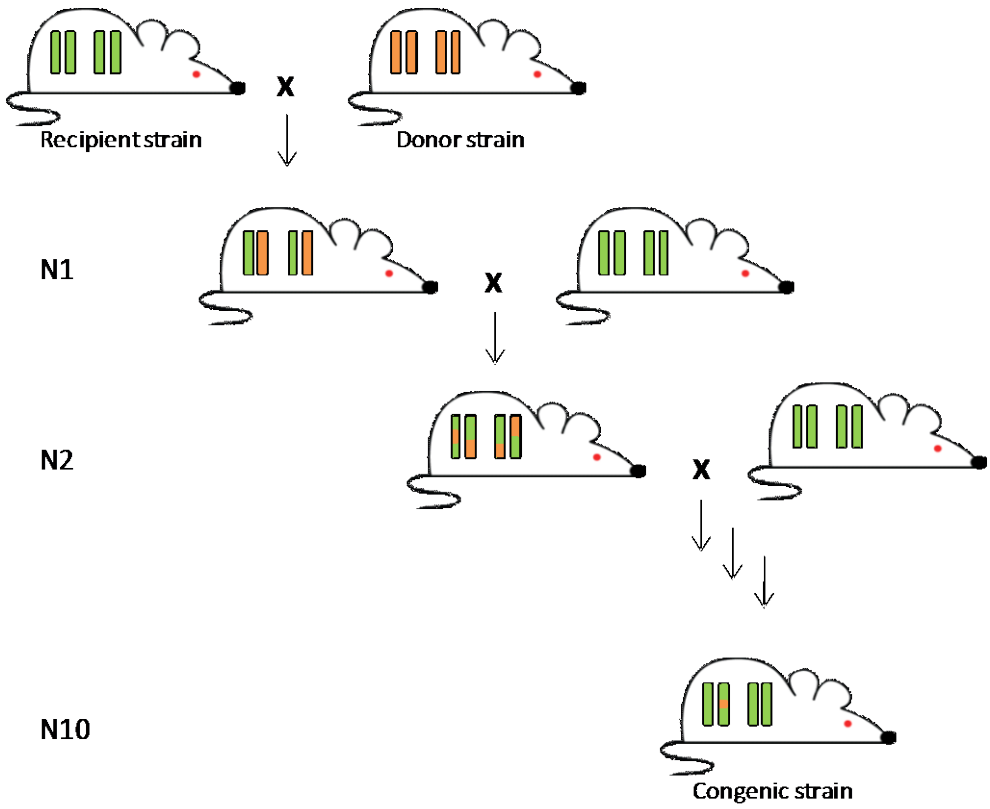

Figure 1.2. Congenic strains. A congenic strain that differs from the recipient strain exclusively in the congenic locus is obtained after serial selected backcrossing to the recipient strain.

1.2.1.3 Identification of candidate genes

Below, a set of criteria proposed by the *Complex Trait Consortium* for the identification of a gene underlying a QTL is listed. To determine the causative gene of a QTL it is not required to cover all the criteria, but it is sufficient to demonstrate a predominance of evidences that support the causative gene [48].

Polymorphism in coding or regulatory sequence. It should be found a correlation between allelic differences affecting structure or regulation in the gene product and strains that differ in the trait.

Gene function. The gene should be involved in a pathway and/or expressed in target cells types or tissues that may explain the phenotype.

In vitro *functional studies.* *In vivo studies* can be replaced by *in vitro* studies. A target cell type or tissue which expresses the putative gene can be cultured *in vitro* and different tests, such as transfection assays, can be performed to demonstrate the influence of the gene in the phenotype.

Transgenesis or knock-ins. The insertion of alternative alleles of the candidate gene in a animal model can be used to demonstrate the effect of the gene on the quantitative trait.

Deficiency-complementation test. A complementation test between a knock-out and strains with allelic variants in the candidate gene can be used to confirm the gene.

Mutational analysis. Gene-specific induced or spontaneous mutations in the candidate gene should affect the quantitative trait.

Homology searches. The mapping of homologous genes or region in humans and mice affecting the same trait is an evidence that gene is involved in the corresponding trait.

1.2.2 QTLs in mouse models of rheumatoid arthritis

To date, more than 80 QTLs controlling different arthritis phenotypes have been identified in RA murine models (reviewed in [49, 56]). These QTLs map along the 20

chromosomes. Several genes have been proposed as candidate genes underlying the QTLs; however in few cases the association has been proven. Some success examples are the MHCII [57, 58], *Ncf1*, *C5* [59, 60] and *Zap70* [61] genes.

Most QTLs have been identified in induced-mouse models such us CIA [59, 62-64], PGIA [65-67], K/BxN serum-transfer arthritis (STIA) [68, 69], and *Borrelia burgdorferi*-associated arthritis [70-72]. Of note, very few QTLs have been identified in spontaneous models such as MRL/lpr mice and BXD2/TyJ mice. In a cross between the MRL/lpr and C3H/lpr strains *Paam1* and *Paam2* QTLs were identified [73] and in a cross between the BXD2/TyJ strain and the parental B6 and DBA/2 strains *Erars1* and *Erars2* QTLs were determined [40].

1.3 Identification of and fine mapping *Cia27*

Identification of *Cia27* - F2 intercross

In CIA as in RA, both MHC genes and non-MHC genes contribute to the susceptibility to disease, as remains proved by the DBA/1J and FVB/N strains. Both strains carry the same susceptible H2-q haplotype; however DBA/1J is highly susceptible to arthritis induction whereas FVB/N is completely resistant to it. In 2004, Bauer et al. [35] used a F2 intercross between DBA/1J and FVB/N strains to indentified QTLs involved in CIA pathogenesis. Further to confirming two QTLs already indentified in previous studies, five new QTL were identified in that study: *Cia27* on chromosome 5 controlling anti-CII IgG2a response; *Cia28* and *Cia29* in chromosomes 13 and 10 respectively, controlling anti-CII IgG1 response; *Trmq3* (T cell ratio modifier QTL3) in chromosome 2, linked to CD4:CD8 ration; and, *Lp1* (lymphocyte proliferation 1) on chromosome 16, linked to cell proliferation.

IgG2a is thought to be one of the main isotypes involved in the pathogenesis of RA [74, 75]. Several QTLs linked with other aspect of the disease were previously indentified on chromosome 5 such as *Cia13* and *Cia14* for CIA [36], *Pgia16* for proteoglycan-induced arthritis [37] and *Bbaa3* and *Bbaa2* for borrelia burgdorferi-

associated arthritis [38], suggesting the relevance of this chromosome in the development of arthritis. However, *Cia27* was the first QTL in chromosome 5 to be linked with anti-CII antibody production. These findings were confirmed few years later in an independent study by Lindvall et al [64] who discovered *Eae39*, a QTL overlapping with *Cia27* which was controlling disease susceptibility and antibody response to CII.

Fine mapping *Cia27* - advanced intercross line

Initially, the confidence interval of *Cia27* was 43 Mbp. To fine map the QTL, an AIL was performed [76]. In this approach, it was confirmed the link of *Cia27* to anti-CII IgG2a response and the QTL was refine into a 4.1 Mbp region. Moreover, *Cia27* was associated with other clinical phenotypes such as susceptibility, severity and onset of disease, with relatively lower LOD scores.

Fine mapping *Cia27* – *in silico* mapping

The region of 4.1 Mbp obtained after the AIL covered 37 genes. To further fine map the QTL, *in silico* mapping was performed. Haplotype blocks were generated with four mouse strains, half of them susceptible to CIA, DBA/1J and B10.D1-H2Q/SgJ (B10q), and half resistant, FVB/N and RIIIS/J. The haplotype blocks which were distinguishable between susceptible strains and resistant strains were considered candidate areas to contain the gene/s underlying the QTL (data not published). As seen in Figure 1.3, six main candidates were pinpointed: *Thrap2* (thyroid hormone receptor-associated protein 2), *Tbx3* (T-box protein 3), *Tbx5* (T-box protein 5), *Rbm19* (RNA binding motif protein 19), *Lhx5* (LIM homeobox protein 5) and *Sdsl* (serine dehydratase-like).

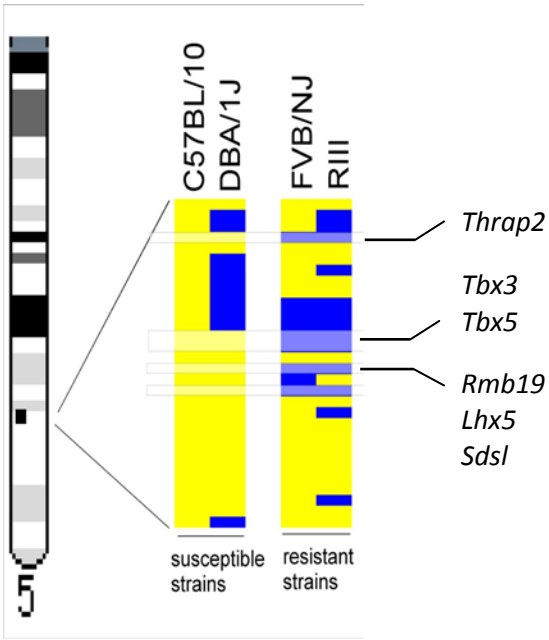

Figure 1.3. *In silico* mapping *Cia27*. Haplotype blocks of the 4.1 Mbp region were generated by 47 SNPs with four mouse strains. The SNP genotype information was retrieved from the mouse resources at Wellcome Trust Centre for Human Genetics (WTCHG) or genotyped by our own group. As reference, B10q strain was used and its alleles are represented in yellow colour. Alleles of other strains are represented in yellow colour when they are the same as B10q alleles; otherwise, they are represented in blue colour.

Fine mapping *Cia27* - congenic strains

To resolve *Cia27* further, a multi-congenic strains approach was used. Donor strains were selected by their allelic heterogeneity on the *Cia27* locus: FVB/N, ALR/LtJ, C3H/HeJ, NOD/ShiLtJ, NZB/BINJ and YBR/EiJ. The congenic fragments were transferred to two CIA-susceptible backgrounds: B10q and DBA/1J.

Mice from the fifth generation (N5) of the congenic strains B10q.FVB-*Cia27*, B10q.ALR-*Cia27*, B10q.NZB-*Cia27*, B10q.YBR-*Cia27,* DBA.FVB-*Cia27* F2 and DBA.FVB-*Cia27* F13 were immunized with CII and a linkage analysis was performed. The result of that study suggested *Thrap2* as a main candidate gene of *Cia27*; however, no significant data was obtained (data not published).

Fine mapping Cia27 - allelic polymorphisms

To explore whether there were change in protein structure of the candidate genes between DBA/1J and FVB/N, the exonic regions were sequenced. Three non-synonymous polymorphisms were identified in *Thrap2* and *Tbx3* genes, resulting in Glu-814-Asp, Thr-950-Met and Val-1222-Ile substitutions in Thrap2 protein, and Glu-306-Asp, Glu-379-Asp and Ala-694-Thr substitutions in Tbx3 protein (data not published).

2 Aim of the study

This thesis focused on the genetic etiology of arthritis in mice and consists of two parts of experiments. In the first part, the aim was to dissect the genetic basis of the arthritis-prone BXD2/TyJ strain, a genetically poorly studied model which has strong similarities with the human RA. The second aim was to fine map the *Cia27* QTL in order to identify the underlying gene. Further, it aimed to elucidate the target cell-type affected by the causal gene and its contribution in the pathology of arthritis.

3 Materials and methods

3.1 Materials

3.1.1 Chemicals and reagents

Accell Delivery Media	Thermo Fisher, Germany
Acetic acid	Merk, Germany
Agarose	Biozyme Scientific, Germany
Bovine Collagen type II 10mg	Mdbioscience, Switzerland
Bovine serum albumin (BSA)	Serva, Germany
Incomplete Freund´s adjuvant (IFA)	DIFCO, USA
dNTP Set, 100mM solutions 4x1 ml	Fermentas, Germany
DreamTaq™ DNA polymerase	Fermentas, Germany
EDTA	Roth, Germany
Ethanol	Roth, Germany
FAST p-Nitrophenil Phosphate Tablets (pNPPM)	Sigma-Aldrich, Germany
Fetal bovine serum (FCS)	PAA Laboratories, Germany
GelStar® Nucleic Acid Gel Stain	Lonza, USA
GenRuler Low Range DNA Ladder	Fermentas, Germany
HPLC-water	Gibco, USA
H_2SO_4	Roth, Germany
KCl	Merk, Germany
KH_2PO_4	Merk, Germany
Methanol	Sigma-Aldrich, Germany
Mycobacterium tuberculi H37 RA	DIFCO, USA
NaCl	Roth, Germany
Na_2HPO_4	Roth, Germany
NaOH	Merk, Germany
Penicillin/Streptomycin	PAA Laboratories, Germany

PBS	Gibco, USA
RNAlater RNA stabilization reagent	Qiagen, Germany
RPMI 1640 medium	PAA Laboratories, Germany
Separation Gel LPA 1, 20 mL	Beckman Coulter, Germany
Separation Buffer	Beckman Coulter, Germany
Sample Loading Solution (SLS)	Beckman Coulter, Germany
TaqMan® Universal PCR Master Mix	Applied Biosystems, USA
TaqMan® Genotyping Master Mix	Applied Biosystems, USA
TMB-ELISA	Thermo Fisher, Germany
Tris-HCl	Roth, Germany
Trypanblue	Biochrom, Germany
Tween 20	Merk, Germany
2-β-Mercaptoethanol	Sigma-Aldrich, Germany

3.1.2 Mediums and buffers

Complete medium	Roswell Park Memorial Institute (RPMI) 1640 medium + 50
µM	2-β-mercaptoethanol + 2 mM L-glutamine + 10 mM HEPES
	+ 100 U/ml penicillin + 100 µg/ml streptomycin + 10% FCS
Media	Accell Delivery Media + 50 µM 2-β-mercaptoethanol
PBS	137 mM NaCl, 2.7 mM KCl, 1.5 mM KH2PO4 and 8.5 mM
	Na_2HPO_4, pH 7.4.
PBS-T	PBS + 0.1% (v/v) Tween 20
TAE	Tris-HCl 10 mM, EDTA 1 mM , pH 8.0
FACS buffer	PBS + 1%BSA
MACS® buffer	PBS + 0.5% BSA + 2 mM EDTA

3.1.3 Oligonucleotides

Subcongenic strain genotyping

D5teschm15 primers were labeled with Cy5 and D5Mit136 were labeled with IRD700. All primers used for genotyping in this study were purchased from Biomers (Germany),

except D5Mit136 which was purchased from Metabiom (Germany). Primer and sequence are listed in Table 3.1; interrogation primers (IP) and restriction enzymes used for genotyping are included.

Table 3.1. Markers for subcongenic strains genotyping

Marker	Sequence	Restriction Enzyme
D5teschm15	FP: 5'-CGTTCCTTCTGCATCTACCC-3'	
	RP: 3'-ACAGTTGTCCCGGTGTGGTA-5'	
rs46503071	FP: 5'-GCTCAGCAGGTCTGTCTTCC-3'	
	RP: 3'-CCACTTGGGAAACCTTGAAA-5'	
	IP: 3'-AGCCTTCCCAAAGCCGCACCCTATTCT-5'	
rs52121564	FP: 5'-GGAACGCCTGAAATAGCATAA-3'	VspI
	RP: 3'-GTGTGTGCGTGTGTGTGTCT-5'	
rs13478485	FP: 5'-CTTTCACACGCAGAGCAGAG-3'	
	RP: 3'-CCACGCATGCCTTAAAAACT-5'	
	IP: 5'-GTGTGTGCTTTAGGTGGACAACAGTGAGATTT-3'	
D5Mit136	FP: 5'-CTTCCAGGATGATTTACAGTATAACTG-3'	
	RP: 3'-AAACTTGCCCACTCCCATC -5'	
rs33215085	FP: 5'-TCCTCGAAGATGAGCTGGAT-3'	
	RP: 3'-CGTGTGCTGATTCTGAAGGA-5'	
	IP: 5'-CGGAAAGCCCCAGAGCCCCCC-3'	
rs36642096	FP: 5'-TCTGTGTTCCGTGTCTCTGC-3'	HhaI
	RP: 3'-GTGCAGGGGTCGTATGTTCT-5'	
	IP: 3'-GGTCGTATGTTCTGACACTGGCTCACTCAG-5'	
rs47812069	FP: 5'-GGAGAAAGTGCTGCCTTCAC-3'	TaqI
	RP: 3'-CTGGAGTCTGCAGGTGTTTG-5'	

FP, forward primer; RP, reverse primer; IP, interrogation primer.

Human genotyping

TaqMan® SNP Genotyping Assay rs10507251 Applied Biosystems, USA

TaqMan® SNP Genotyping Assay rs17580303	Applied Biosystems, USA
TaqMan® SNP Genotyping Assay rs9788041	Applied Biosystems, USA

Quantification of gene expression by real-time PCR

The following validated assays contain a pair of unlabeled PCR primers and a dye-labeled TaqMan® probe:

TaqMan® Rodent GAPDH Control Reagent (VIC™ Probe)	Applied Biosystems, USA
TaqMan® Gene Expression Assay Med13L	Applied Biosystems, USA
TaqMan® Gene Expression Assay Tbx3	Applied Biosystems, USA
TaqMan® Gene Expression Assay Tbx5	Applied Biosystems, USA
TaqMan® Gene Expression Assay Rbm19	Applied Biosystems, USA
TaqMan® Gene Expression Assay Lhx5	Applied Biosystems, USA
TaqMan® Gene Expression Assay Sdsl	Applied Biosystems, USA

3.1.4 Enzymes

DreamTaq DNA Polymerase	Fermentas, Germany
Shrimp Alkaline Phosphatase (SAP)	Fermentas, Germany
Exonuclease I (Exo)	Fermentas, Germany
VspI (AseI)	Fermentas, Germany
FastDigest® HhaI	Fermentas, Germany
FastDigest® TaqI	Fermentas, Germany

3.1.5 Antibodies

Purified Anti-mouse CD3	BD Pharmingen, USA
Purified Anti-mouse CD28	BD Pharmingen, USA
Purified Anti-mouse IgM+IgG+IgA(H+L)	Southern Biotech, USA
Anti-mouse CD16/CD32 (Mouse BD Fc Block™)	BD Pharmingen, USA
FITC Anti-mouse CD4	BD Pharmingen, USA
FITC Anti-mouse CD45R (B220)	eBioscience, Germany
PE Anti-mouse CD8	BD Pharmingen, USA

PE Anti-mouse CD23	eBioscience, Germany
PE Anti-mouse CD11b	BD Pharmingen, USA
PE Anti-mouse F4/80	Caltag Lab, UK
PE Anti-mouse CD138	BD Pharmingen, USA
APC Anti-mouse CD3e	BD Pharmingen, USA
Cy5 Anti-mouse CD21	eBioscience, Germany
A647 Anti-mouse CD11c	eBioscience, Germany
Biotin Hamster Anti-Mouse TCR β Chain	BD Pharmingen, USA
Biotin Rat Anti-Mouse CD45R/B220	BD Pharmingen, USA
Rat Anti-mouse Ki-67 Antigen	DakoCytomation, Denmark
Alkaline Phosphatase-conjugated Goat Anti-mouse IgG2a	Bethyl, USA
Alkaline Phosphatase-conjugated Goat Anti-mouse IgG2c	Southern Biotech, USA
Alkaline Phosphatase-conjugated Polyclonal Rabbit Anti-mouse IgG	Jackson ImmunoResearch, UK
HRP-conjugated Polyclonal Rabbit Anti-mouse IgG1	BD Pharmingen, USA
7-AAD	BD Pharmingen, USA

3.1.6 Commercial kits

B Cell Isolation Kit, mouse	Miltenyi Biotec, Germany
$CD4^+$ T Cell Isolation Kit II, mouse	Miltenyi Biotec, Germany
DNA Size Standard Kit - 400 Base Pairs	Beckman Coulter, Germany
DNA Size Standard kit- 80 Base Pairs	Beckman Coulter, Germany
GeneJET™ Gel Extraction Kit	Fermentas, Germany
GenomeLab™ SNPStart Primer Extension Kit	Beckman Coulter, Germany
First Strand cDNA Synthesis Kit	Fermentas, Germany
RNeasy Mini Kit	Qiagen, Germany
DNeasy Blood & Tissue Kit	Qiagen, Germany
QIAamp DNA Blood Mini Kit	Qiagen, Germany

3.1.7 Transfection reagents

Accell SMART pool siRNA, mouse THRAP2	Thermo Fisher, Germany
Accell Non-Targeting siRNA	Thermo Fisher, Germany
Accell Green Non-Targeting siRNA	Thermo Fisher, Germany
Accell GAPDH Control siRNA, mouse	Thermo Fisher, Germany

3.1.8 Laboratory supplies

Cell culture flasks	Sarstedt, Germany
Beckman Coulter 96-well plates	Beckman Coulter, Germany
DNA Separation Capillary Array, 33 cm x 75 µm	Beckman Coulter, Germany
MACS® Separator Columns, LS Columns	Miltenyi Biotec, Germany
Micro-emulsifying needles 18x1-7/8 (47.6MM)	Popper, USA
Microtiter plates (96-well, flat bottom)	Nunc, Germany
Mictotiter plates (96-well, round bottom)	Greiner bio-one, Germany
Multiply®-µStrip Pro 8-strip PCR tubes	Sarstedt, Germany
Pipet (5, 10, 25 ml)	Sarstedt, Germany
Pipet tips	Sarstedt, Germany
Pipet filter tips	Sarstedt, Germany
Plastic tubes (15 ml, 50 ml)	Sarstedt, Germany
Reaction tubes (0.5, 1.5, 2 ml)	Sarstedt, Germany
RNase-free tubes (1.5 ml)	Sarstedt, Germany
RNase-free pipet filter tips	Sarstedt, Germany
Round-bottom FACS tubes (5 ml)	Becton Dickinson, USA
Sample microtiter plates, 25/pk	Beckman Coulter, Germany
Tissue culture plates (96-well, flat bottom)	Sarstedt, Germany
96 Multiply® PCR plate	Sarstedt, Germany
BD Vacutainer® Blood Collection Tubes	Becton Dickinson, USA
PALM® MembraneSlides, 1 mm	Carl Zeiss, Germany

3.1.9 Instruments

Centrifuge 5810R	Eppendorf, Germany
CEQ/GenomeLab Genetic Analysis System, CEQ^{TM}8800	Beckman Coulter, Germany
C1000 Thermal Cycler	BioRad, USA
EW-N/EG-N Precision Balance	Kern, Germany
Microfuge 22R Centrifuge	Beckman Coulter, Germany
MidiMACS™ Separator	Miltenyi Biotec, Germany
Mikro 120, Microcentrifuge	Hettich, USA
Mini Centrifuge MCF-2360	LMS, Japan
Minifuges™	Labnet International, USA
Pipetus	Hirschmann, Germany
Precision pipet set (10/20/100/200/1000 µl)	Eppendorf, Germany
PowerPac Basic, Power Supply	BioRad, USA
Sterile Hood HeraSafe	Heraeus, Germany
Thermomixer Compact	Eppendorf, Germany
Vortexer Heidolph REAX 2000	Heidolph, Germany
2720 Thermal Cycler	Applied Biosystems, USA
ELISA PLATE washer	TECAN, Switzerland
VICTOR3 Wallac 1420	Perkin-Elmer LAS, Germany
Nanodrop 2000c	Thermo Fisher, Germany
Mastercycler EP Gradient	Eppendorf, Germany
PALM MicroBeam	Zeiss microImaging, Germany

3.2 Methods

3.2.1 Mouse models

3.2.1.1 Spontaneous arthritis

Mice used in this study were housed under climate-controlled conditions with 12-h light/darkness cycles at the animal facility at the University of Rostock. The procedures

were approved by the governmental administration of the State of Mecklenburg-Vorpommern.

3.2.1.1.1 Generation of four-way AIL

An outbred four-way autoimmune-prone advanced intercross line (AIL) was originated by our group from the parental mouse strains BXD2/TyJ, MRL/MpJ, NZM2410/J and Cast. The four inbred strains were intercrossed following an equal strain and sex distribution. At each time, 50 breeding pairs were used to generate the next generation. Parental strains were acquired from Charles River Laboratories, Germany.

3.2.1.1.2 Clinical status monitoring

A total of 366 mice from the fourth generation (G4) of the four-way autoimmune-prone AIL were scored for development of spontaneous arthritis. Mice were assessed twice per week to measure onset and evolution of clinical disease according to a scoring system based on the number of inflamed joints. Each paw was scored individually, each inflamed toe and knuckle was given a score of 1, and an inflamed wrist or ankle was given a score of 5; maximum score of 15 per limb and of 60 per mouse.

3.2.1.2 Collagen-induced arthritis

Mice used in this study were housed under climate-controlled conditions with 12 h light/darkness cycles at the animal facility at the University of Lübeck. The procedures and assays were approved by the governmental administration of the State of Schleswig-Holstein.

3.2.1.2.1 Generation of subcongenic strains

The B10.D1-H2q/SgJ (B10q) strain and the B10.RIII-*Eae39* C19 (C19) and B10.RIII-*Eae39* C20 (C20) subcongenic strains were kindly provided by Prof. R. Holmdahl (Karolinska Institute, Sweden) and were bred in the animal facility at the University of Lübeck. The C19 and C20 subcongenic strains were generated by marker selected backcrossing of

the RIIIS/J donor strain to the B10.RIII recipient strain as reported in Lindvall et al. [64]. In our facility, C19 and C20 heterozygous mice were intercrossed and genotyped to generate C19 and C20 homozygous mice, respectively, and subsequently the C19/C20 heterogeneous subcongenic strain.

The B10q.C3H-*Cia27* (B10q.C3H) subcongenic strain was created by followed backcrossing of the previously produced B10q.C3H congenic strain into the B10q background. Homozygous B10q.C3H mice carry two alleles from the C3H/HeJ strain in the *Cia27* locus, and hold different alleles in *Thrap2* than B10q mice.

3.2.1.2.2 Induction of disease

CIA was induced in 8 - 12 weeks old mice by intra-dermal immunization at the base of the tail with 125 µg bovine type II Collagen (CII) (2.5 mg/ml in 0.1 M acetic acid) previously emulsified with micro-emulsifying needles in an equal volume of complete Freund's adjuvant (CFA) (Incomplete Freund´s adjuvant (IFA) + 4 mg/ml *Mycobacterium tuberculosis*) and, in certain experiments, subsequently boosted at day 40 with 125 µg bovine CII emulsified in IFA.

3.2.1.2.3 Clinical status monitoring

Arthritis development in CII-immunized mice was assessed as described in section 3.2.1.1.2.

3.2.1.2.4 Sacrificing and sampling

Mice were sacrificed ~60 days post-immunization. Once sacrificed, necropsy was performed and blood, spleen and lymph nodes (LN) samples were taken. Serum was obtained from blood samples after centrifugation at 14,000 rpm 10 minutes (min) at 4°C and stored at 20°C. Spleen was processed for flow cytometry as described in paragraph 4.2.5. LN samples were submerged in RNA*later* immediately after harvesting and stored at -20°C.

3.2.1.3 OVA immunization

Ovalbumin (OVA) emulsified with aluminum (alumOVA) is a widely used model for T cell-dependent immunization. Mice were intra-peritoneally immunized with 100 µl of alumOVA containing 50 µg OVA emulsified with micro-emulsifying needles in an equal volume of aluminium. In total, 5 B10q.C3H subcongenic mice and 5 wildtype B10q mice were immunized in two independent experiments. Mice were sacrificed at day 10 post-immunization and spleen biopsies were microdissected (see 3.2.7).

3.2.2 Genotyping

3.2.2.1 DNA isolation

Genomic DNA from tails biopsies of mice was isolated by incubation in 500 µl 50mM NaOH at 95°C for 2 hours (h), and posterior addition of 50 µl 1M Tris-HCl (pH 8.0). For genotyping with Illumina Mouse High Density array, pure genomic DNA was isolated with the DNeasy Blood & Tissue Kit according to manufacturer's instructions.

3.2.2.2 Four-way AIL Mice genotyping and association analysis

Illumina Mouse High Density array was used to genotype 1,400 SNPs from 366 G4 mice. The association analysis was performed by the R version of HAPPY as described in [77] on Debian Linux [78]. In brief, the founder haplotype structure for each mouse is inferred by the HAPPY algorithm taking into account the adjacent markers. QTLs then are detected by a regression model applied to the inferred haplotypes in the intervals between adjacent markers. The association seeks for differences between the genetic effects of the parental haplotypes. This association provides ANOVA significance levels, presented as the negative base-10 logarithmic *P* value (-log *P*), which are considered theoretical values. To determine the empirical threshold for statistical significance, 1,000 permutations were performed [77]. In permutation tests the assignment of phenotypes to individuals is shuffled prior to every ANOVA association. The empirical *P* value is then given by the percentage of runs for which the *P* value obtained at each position is greater than the *P* value initially obtained on the real data. Empirical

significance thresholds was established at $P < 0.01$ for each phenotype. Data from all chromosomes were analyzed simultaneously with an additive model, which assumes that the contribution of each allele at the locus is additive. Confidential intervals (CI) of QTLs were estimated manually to comprise the region around a peak up to a drop of the *P* value by $P < 0.05$. Gender was used as covariate.

Some of the mice in this work were simultaneously assessed for EBA development for an independent study, and therefore immunized with type VII collagen (CVII) [82]. To exclude a bias in the analysis, CVII immunization was also included as covariate.

3.2.2.3 Subcongenic strains genotyping

Microsatellites

Two microsatellite markers were genotyped by polymerase chain reaction (PCR) amplification as follows: 2 µl of genomic DNA was amplified in a final volume of 10 µl containing 0.25 U DNA polymerase, 1 µM primers and 0.25 mM dNTP. The following thermal cycling program was applied: 95°C for 3 min, followed by 36 cycles of 95°C for 30 seconds (s), 56°C for 30 s and 72°C for 1 min, and a final extension at 72°C for 10 min.

PCR products were separated and detected by capillary electrophoresis with the CEQ System Fragment Analysis module of the CEQ^{TM}8800 (CEQ). Sample preparation for loading onto the CEQ was performed as follows: 3 µl PCR product was added to 23 µl SLS including 0.4 µL CEQ400 size standard mixture, and covered with one drop of mineral oil.

SNP genotyping: single-base extension method

Four SNPs were genotyped by single-base extension technology (Table 3.1). Prime extension products were created by hybridization of unlabeled interrogation primer (IP) to previously created PCR templates followed by single-base extension of fluorescent dye labeled terminator dNTPs. The extended fragments were then combined with the

size standard 80 and loaded onto the CEQ for automated separation and detection. PCR was performed as described in Microsatellite Marker Genotyping section adjusting the annealing temperature to the primers used. To clean out the excess primers, single-stranded DNA and dNTPs, PCR products were purified by Exo/SAP digestion: 10 U Exo and 2 U SAP were added to 5 µl PCR product and incubated for 15 min at 37°C and 15 min at 65°C. SNP-primer extension reaction was then performed: 1 µl purified PCR product was mixed with 3 µl SNPStart MasterMix (provided in the GenomeLab™ SNPStart Primer Extension Kit) and 1 µM IP in a final volume of 10 µl, and amplified in a 2-step protocol: 90°C for 10 s followed by 45°C for 20 s and repeated for 25 cycles. Next, to eliminate unincorporated dye terminators 0.25 U SAP was added to the primer extension product in a final volume of 13 µl and incubated 30 min at 37°C followed by 15 min at 65°C. Finally, to load onto the CEQ samples were prepared as described above. CEQ80 size standard mixture was used for SNP genotyping.

SNP genotyping: RFLP method

By restriction fragment length polymorphism (RFLP) method, three SNPs were genotypes (Table 3.1). PCR products were digested by restriction enzymes following the instruction of the manufacturer. Enzymes were chosen regarding their capacity to differentiate between the polymorphic alleles of the parental strains. Digestion products were visualized in 2% agarose gels.

3.2.3 Gene expression analysis

3.2.3.1 RNA isolation

Total RNA was isolated from cells using the RNeasy Mini or Micro Kit, depending on the amount of cells, according to manufacturer's instructions. Briefly, an appropriate amount of cells was pellet and resuspended in a suitable amount of RLT buffer containing 1% v/v 2-β-mercaptoethanol. Cells were disrupted by pipeting and one volume of 70% ethanol was added to the homogenized lysate. Sample was transferred to a gDNA column for DNA removal. Flow-through was transferred to RNeasy spin

column placed in a 2 ml collection tube and centrifuged for 15 s at 14,000 rpm. Next, in consecutive steps, RW1 and RPE buffers were added, and flow-through was discarded after centrifugation. Finally, RNA was eluted from the column with 14 - 30 µl RNase-free water (for Micro and Mini kit, respectively) by centrifugation. All materials used in this process were RNase-free. RNA concentration was measured by NanoDrop.

3.2.3.2 Reverse transcription

cDNA was synthesized from total RNA by reverse transcription using the First Strand cDNA Synthesis Kit. Total RNA (between 0.1 ng - 1 µg) was mixed with 1 µl random hexamer primer, 4 µl 5X Reaction Buffer, 2 µl 10 mM dNTP Mix, 1 µl RiboLock RNase Inhibitor (20 U/µl), 1 µl RevertAid M-MuLV Reverse Transcriptase (200 U/µl) in a total volume of 20 µl. Templates were incubated for 5 min at 25°C followed by 60 min at 42°C and 5 min at 70°C.

3.2.3.3 Quantitative real-time PCR

Mastercycler EP Gradient real-time PCR system was used for quantitative real-time PCR analysis. PCR reactions contained 1X TaqMan® Gene Expression Assay (or 100 nM of Rodent GAPDH Primes and 200 nM of Rodent GAPDH Probe (VIC), in the case of *Gapdh* gene), 1X TaqMan® Universal PCR Master Mix and 1 µl cDNA. Absolute threshold cycle (Ct) values were determined with the Mastercycler ep CycleManager software version 1.2.0 (Eppendorf). mRNA expression was normalized to the housekeeping gene (HKG) *Gapdh* or *Mln51* by applying the equation: $2^{(\text{ct gene-ct HKG})}$ [77].

3.2.4 Flow cytometry

Single cell suspensions preparation

Spleen was excised, suspended through a 70 µm nylon cell strainer and washed twice in PBS. Cells were centrifuged at 300 g for 10 min and resuspended in a suitable amount of flow cytometry buffer (FACS buffer).

Surface staining and data acquisition

Cell density was adjusted to 10^6 or 10^8 cell/100 µl for acquisition or sorting, respectively. Cells were incubated for 5 min at 4°C with anti-CD16/CD32 (1 µg/ml) to block FcγR-mediated binding. Next, cells were stained for 20 min at 4°C with antibodies (0.5 - 2 µg/ml). Cells were washed twice and resuspended in 300 - 500 µl of FACS buffer. For identification of dead cells, samples were incubated with 4',6-diamidino-2-phenylindole (DAPI) or 7-Amino-Actinomycin D (7-AAD) 2 min or 10 min before analysis, respectively. Data was acquired on Calibur or LSRII flow cytometers and analyzed using the FlowJo software. For sorting, cells were resuspended in 500 µl of FACS buffer and sorted in the MoFlo High Speed Cell Sorter in the Core Facility Cell Sorting of the University of Lübeck.

3.2.5 ELISA

To measure the specific antibody production against CII, enzyme-linked immunosorbent assay (ELISA) was used. A pool of positive sera was used as standard. ELISA was preformed as described below. The amounts detailed in the protocol are per well; washing steps were performed three consecutive times with the ELISA PLATE washer by adding 200 µl PBS-T.

96-well flat-bottom microtiter plates were coated with 50 µl bovine CII (5 µg/ml in PBS) and incubated over night at 4°C. After washing, plates were blocked with 100 µl 1% BSA/PBS-T and incubated with agitation for 1 h at room temperature (RT). Next, plates were washed and 50 µl serum samples or standard were applied in duplicates. Serums and standard were previously diluted (1:50, 1:500 and 1:5,000 dilution for serum samples and 1/50, 1/250, 1/1,250, 1/6,250, 1/31,250, 1/156,250 for standard) in 1% BSA/PBS-T in a 96-well round-bottom low-binding microtiter plates. After 2 h of incubation at RT with agitation, plates were washed. Next, 50 µl previously diluted enzyme-conjugated antibodies were added and incubated with agitation for 1 h at RT. Antibodies were used diluted in PBS as follows: 1:6,000 anti-mouse IgG2a-AP, 1:4,000

anti-mouse IgG2c-AP, 1:8,000 anti-mouse IgG-AP, and 1:10,000 anti-mouse IgG1-HRP. After a last washing step, developing was performed. For antibodies AP-conjugated, 50 µl pNNTT was added as enzyme substrate and incubated for 5 - 20 min at RT. Reaction was stopped with 20 µl 1M NaOH. In the case of HRP-conjugated antibody, 50 µl TMB was added and after 4 min incubation, reaction was stopped with 50 µl of 1 M H_2SO_4. The measurement of optical density (OD) was accomplished in a 96-well photometric detector VICTOR3 at the wavelength of 405 or 450 nm, respectively.

Blank-subtracted OD-values were used for calculation of relative concentrations. Softmax was used to calculate the 4-parameter curve fitting and data was analyzed with EXCEL.

3.2.6 *In vitro* experiments

Cells were isolated and cultured under sterile conditions in a laboratory hood. All cell cultures were incubated in 96-well plates at 37°C and 5 % CO_2.

3.2.7 Lymphocyte isolation

Single cell suspension was generated from spleen and lymph nodes by gentle mechanical dissociation between two glass slides and then filtered through a cell strainer. Mouse B and CD4 T lymphocytes were isolated by magnetic cell separation, MACS® technology, using the B Cell and $CD4^+$ T Cell Isolation Kits according to manufacturer's instructions.

3.2.8 Culture and stimulation

B cells were cultured in 100 µl Accell delivery media supplemented with 50 µM 2-β-mercaptoethanol (media). When indicated, media was supplemented with 10% or 3% FCS and 100 µl fresh media was added. For stimulating B cell, cells were cultured in presence of the following stimuli: LPS (50 µg/ml or 10 µg/ml), anti-Ig (2 µg/ml) or plate-bound anti-CD40 antibody (0.5 µg). For anti-CD40 stimulation, prior to seeding the cells, plates were coated with 50 µl anti-CD40 (10 µg/ml in PBS) during 1 h at RT, and then

washed twice with 200 µl PBS. T cells were stimulated with plate-bound anti-CD3 antibody (0.25 µg) and soluble anti-CD28 antibody (2 µg/ml). Prior to seeding the cells, plates were coated with 50 µl anti-CD3 antibody (5 µg/ml in PBS) over night at 4°C, and then washed twice with 200 µl PBS.

3.2.9 Knockdown assays

Accell SMARTpools siRNA contain four different siRNA to reduce off-target effects and are designed to delivery to hard-to-transfect cells. One µl/100 µl Thrap2 predesigned Accell SMARTpool siRNA or Accell Non-targeting siRNA was delivered into B cells and T cells in the media. Delivery efficiency was previously determined to be ~80% using Non-targeting FITC-labeled control siRNA.

3.2.10 Cell death assessment

Cell death was assessed by 7-AAD or DAPI by FACS. The percentage of specific cell death was calculated as follows:

$$Specific\ cell\ death = 100 \times \frac{\%\ dead\ cells - \%\ baseline\ dead\ cells}{100\% - \%\ baseline\ dead\ cells}$$

where % baseline dead cells is the % dead cells in non-transfected cells [78].

3.2.11 Laser capture microdissection

Spleen biopsies were excised, snap-frozen in liquid nitrogen and stored at -80°C. Biopsies were cut into 10 µm cryosection in a microtome. Cryosections were placed on PALM membrane-covered slides 1 mm for laser capture microdissection (LCM) or on usual glass slides for histology, and stored at -80°C. Next, staining with toluidine blue was performed with the Histogene® LCM Frozen Section Staining Kit according to manufacturer's instruction. To identify the T and B cell compartments in the spleen, the cryosections were stained immunohistologically with biotinylated monoclonal antibody

(mAb) TCR-β or mAb B220, respectively. To visualize proliferating cells and germinal centers, the cryosections were stained for Ki-67 Antigen.

Periarteriolar lymphatic sheath (PALS; or T cell zone), marginal zone (MZ), B cell follicles (FO) and red pulp (RP) compartments were dissected by LCM using a pulsed UV laser Palm MicroBeam. An area of $2x10^6$ μm^2 was microdissected per compartment, immediately dissolved in 350 µl lysis buffer containing guanidinium-isothiocyanate and stored at -20°C. RNA extraction was performed with the RNeasy Kit according to manufacturer's instructions.

3.2.12 Human association study

3.2.12.1 Case-control cohort

The dataset consisted of a total of 358 RA cases and 323 unrelated healthy controls matching in age and sex. Control and case samples were collected from Metropolitan area (Cairo and Giza governorates), Nile Delta and south of Egypt. All samples were from individual with Egyptian ancestry aged between 18 and 75 years. Case samples met the 1987 ACR diagnostic criteria for RA; subjects with psoriasis, SLE and inflammatory bowel disease (IBD) were excluded. All individuals were enrolled with informed written consent.

Peripheral blood was collected in BD Vacutainer® Blood Collection in presence of EDTA, and genomic DNA was extracted with QIAamp DNA Blood Mini Kit according to manufacturer's instructions. DNA concentration was assessed by NanoDrop and quality was determined by DNA electrophoresis on 0.8% agarose gel.

3.2.12.2 SNP genotyping

Human SNPs genotyping was carried out using 1X TaqMan® SNP Genotyping Assay (rs10507251, rs17580303 and rs9788041), 1X TaqMan® Genotyping Master Mix and 10 ng genomic DNA, in a total reaction volume of 10 µl. Amplification was performed on Mastercycler EP Gradient real-time PCR system. Thermal cycle conditions were 50°C for

2 min, 95°C for 10 min, 40 cycles of 95°C for 15 s and 60°C for 1 min. Completed PCRs were analyzed using the Mastercycler ep CycleManager software version 1.2.0.

3.2.13 Statistical analysis and graphic presentation

All data was acquired with the respective equipment, exported to and stored in Excel. Data was analyzed for statistical significance with SigmaPlot 12.0 or with HAPPY (see section 3.2.2.2.). Scientific data and schemes were created and visualized using SigmaPlot 12.0, Powerpoint and LibreOffice Draw 3.5.

4 Result

4.1 Identification of QTLs in a spontaneous arthritis model

To investigate the genetic basis of the arthritic spontaneous BXD2/TyJ mice, 366 G4 mice of the four-way autoimmune-prone AIL were monitored during 6 months for clinical arthritis. G4 mice developed arthritis with a higher incidence in males (85.8%) than in females (57.3%); however, both males and females had similar onset, which reflects the speed of disease progression, and severity of disease, which is measured as maximum score (Table 4.1). The G4 mice of this cross also developed autoimmune pancreatitis [79] and lupus nephritis (data not published).

Table 4.1. Phenotypic characteristics of spontaneous arthritis in G4 mice from the four-way autoimmune-prone AIL

	Incidence	**Onset**[a]	**Maximum score**[b]
Females	113/197	22.9 ± 0.4	4.5 ± 0.4
Males	145/169	21.9 ± 0.4	6.9 ± 0.4
Total	258/366	22.3 ± 0.3	5.6 ± 0.3

a. Onset measured in weeks. Mean ± standard error of the mean (SEM); only disease mice were included in the calculation.

b. Mean ± SEM; all immunized mice were included in the calculation.

The genetic control of susceptibility, onset of disease and maximum score was analyzed by an association study performed with the software package HAPPY algorithm. Statistical significance based on ANOVA test (-log *P*) are provided in Tables

4.2, 4.3 and 4.4. Empirical significance levels were also assessed by 1,000 permutations for every SNP. The empirical *P* values were slightly different than their theoretical values, which indicates that the theoretical *P* values are considerably reliable. A cutoff of 0.01 in the empirical *P* value, equivalent to one false positive per 100 associated SNPs, was defined and those SNPs greater than this threshold were considered significant (Table 4.2, 4.3 and 4.4). In addition, QTLs whose peaks exceeded the $P < 0.001$ threshold are indicated.

Plots of results are represented in Figure 4.1. Fourteen loci were significantly associated with susceptibility to disease on chromosomes 1, 3, 4, 5, 7, 13, 16, 18, 19, and X (Table 4.2); 8 loci were associated with maximum score on chromosomes 1, 4, 7, 13, 18, and 19 (Table 4.3); and 7 loci were associated with onset of disease on chromosomes 1, 3, 7, 11, 13 and 18 (Table 4.4). Interestingly, on chromosome 1 and on chromosome 18 it was found one QTL controlling the three phenotypes. QTLs regulating both susceptibility and maximum score were found on chromosomes 13 and 19, while one QTL controlling susceptibility and onset of disease was identified on chromosome 3. Out of 22 QTLs, 13 were located in previously mapped arthritis QTLs and 11 in regions associated with other autoimmune QTLs (Table 4.2, 4.3 and 4.4). Six QTLs mapped on loci without previously mapped arthritic QTLs, while 3 QTLs spanned regions without previously mapped autoimmune QTLs.

Susceptibility to disease was the phenotype which was most genetically controlled. Four of the 14 identified QTLs showed significant association $P < 0.001$. These QTLs mapped on chromosome 3 (peak in rs3659988; ~6 Mbp CI), chromosome 7 (peak in rs3707067; ~46 Mbp CI), chromosome 13 (peak in rs13481764; ~17 Mbp CI), and chromosome 18 (peak in rs13483426; ~17 Mbp CI) (Table 4.2). Two out of the 8, loci associated with maximum score achieved high significance on chromosome 13 (peak rs13481764; ~12 Mbp CI) and on chromosome 19 (peak in rs6194426; ~11 Mbp CI) (Table 4.3). Regarding onset of disease, one locus on chromosome 7 obtained high level of significance (peaks in rs4226783 and CEL.7_77850273; ~42 Mbp CI) (Table 4.4).

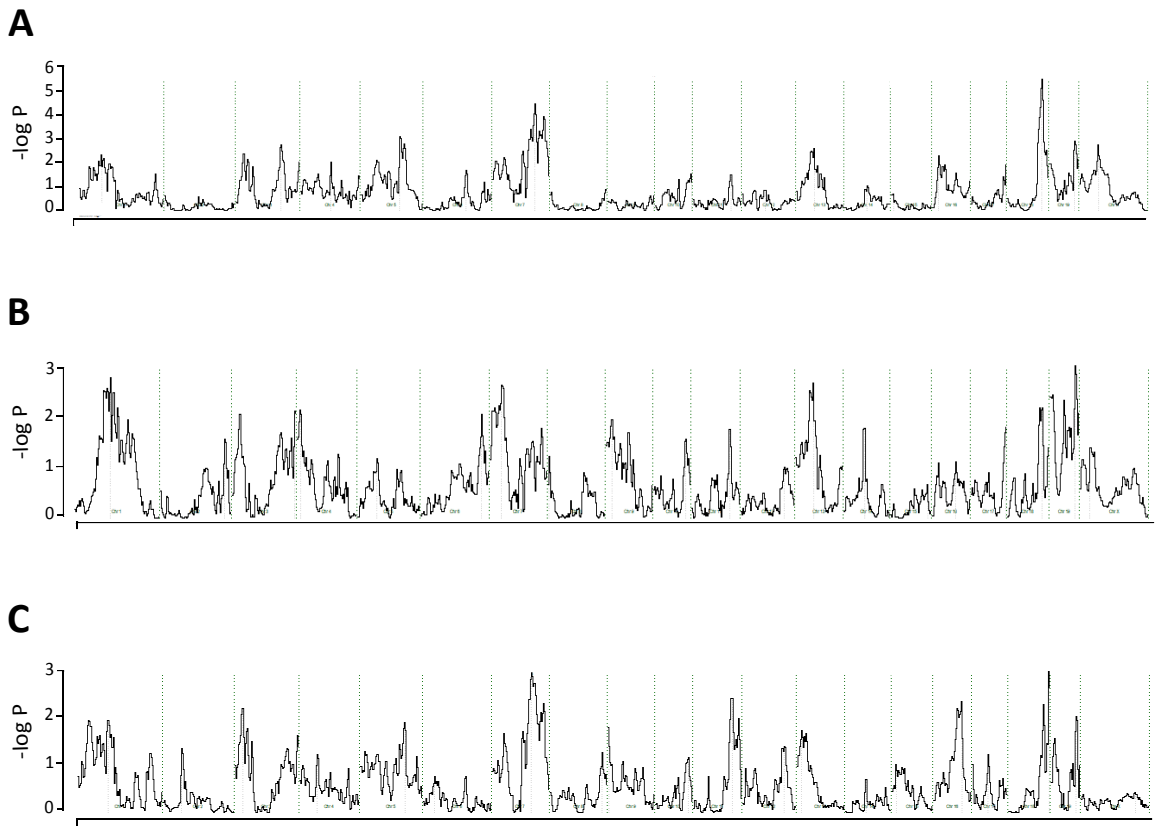

Figure 4.1. Whole-genome linkage map for spontaneous arthritis traits. The x-axis represents position in Mbp and the y-axis shows the ANOVA -log *P* value of association. QTLs controlling susceptibility to disease (**A**), maximum score (**B**) and onset of disease (**C**). Gender and CVII immunization were used as covariates.

Table 4.2. Identified QTLs controlling susceptibility to disease

Chr	Peak	Position (bp[a])	-log *P*[b]	CI	Overlapping arthritis QTL[c]	Overlapping autoimmune QTL[c]
1	rs13475847	45,96	2.4	gnf01.036.770-rs6386920	*Pgia1*	*Psrs4, Idd26*
1[d]	rs6353774	59,77	1.9	rs13475881-rs6288543	*Cia15*	*Eae30, Aec2, Idd5a*
3[d]	rs3659988	16,35	2.3**	rs6248752-rs6235984		
3	rs3660588	30,22	2.1	rs13477030-rs13477043		*Eae20*
3	rs3701653	103,43	2.7	rs3726226-rs3708412	*Cia21, Cia22, Pgia25, Trmq6 mCia2*	
4	rs13477774	73,20	2.0	rs6222684-rs13477774		
5	rs6341620	37,49	2.0	rs3696671-rs13478205		
5	rs13478402	96,61	3.0	rs13459087-rs13459186	*Bbaa3, Eae39, Lctlp2, Pgia16*	*Cypr3, Lmb2*
7	rs13479338	81,20	2.4	rs3676254-rs13479355	*Cia41*	
7[d]	rs3707067	105,86	4.4**	rs6213614-rs3716088	*Cia7, Pgia3, Pgia21*	*Eae4, Nba3, Eae26, Il4ppq*
13[d]	rs13481764	36,64	2.3**	rs6275055-rs13481783		*Bxs6, Idd14*
16	rs4165440	24,17	2.2	rs4165081-rs4177651		
18[d]	rs13483436	64,67	5.4**	rs3688789-rs13483466	*Pgia11, Cia18*	*Eae25, Pgis1, Idd21.1,Lbw6*
19[d]	rs6194426	50,20	2.8	rs3023496-rs6191324	*Paam2*	*Eae19*
X	rs3157124	68,69	2.7	rs13483765-rs3725966	*Pgia24*	

a. Position according to the NCBI Build 37.

b. Significance level determined by ANOVA.

c. QTLs retrieved from MGI database.

(http://www.informatics.jax.org/searches/allele_form.shtml).

d. QTLs controlling more than one phenotype.

All QTLs shown have passed the 0.01 significant threshold by 1,000 permutation test. ** indicates QTLs that have passed the 0.001 threshold. Chr, chromosome; CI, confidential interval; bp, base pair.

Table 4.3: Identified QTLs controlling maximum score

Chr	Peak	Position (bp[a])	-log *P*[b]	CI	Overlapping arthritis QTL[c]	Overlapping autoimmune QTL[c]
1[d]	rs13475919	73,02	2.7	rs13475881-rs6195073	*Cia14, Cia15*	*Eamcd1, Baa2, Aec2, Cdcs2, Eae30, Idd5a*
4	rs3660863	7,12	2.1	rs3695715-UT.4.10.84692		
7	rs4226499	29,61	2.6	rs3714915-rs4232449		
13[d]	rs13481764	36,64	2.6**	rs6275055-rs13481783		*Bxs6, Idd14*
18[d]	rs13483436	73,59	2.2	rs3691542-rs13459193	*Pgia11*	*Eae25, Pgis1, Idd21.1, Lbw6*
19	CEL.19_5283144	5,49	2.4	rs3671671-rs13483525	*mCia12*	
19[d]	rs6194426	50,20	3.0**	rs3023496-rs6191324	*Paam2*	*Eae19*

a. Position according to the NCBI Build 37.

b. Significance level determined by ANOVA.

c. QTLs retrieved from MGI database.

(http://www.informatics.jax.org/searches/allele_form.shtml).

d. QTLs controlling more than one phenotype.

All QTLs shown have passed the 0.01 significant threshold by 1,000 permutation test. ** indicates QTLs that have passed the 0.001 threshold. Chr, chromosome; CI, confidential interval; bp, base pair.

Table 4.4: Identified QTLs controlling onset of disease

Chr	Peak	Position (bp[a])	-log *P*[b]	CI	Overlapping arthritis QTL[c]	Overlapping autoimmune QTL[c]
1[d]	rs6353774	59,77	1.9	rs13475881-rs13475919	*Pgia1*	*Eae30, Aec2, Idd5a*
3[d]	rs3659988	16,35	2.1	rs13476969-rs6235984		
7	rs4226783	100,08	2.9**	rs6213614-rs13479506	*Cia7, Pgia3, Pgia21*	*Eae4, Nba3, Eae26, Il4ppq*
11	rs13481161	92,32	2.4	rs3719581-rs6393948	*Cia40, Cia28*	*Bxs6*
13	rs4197150	66,29	2.1	rs4189277-rs3718160		*Eae13*
18[d]	rs13483436	73,59	2.3	rs6161154-rs13459193	*Pgia11*	*Eae25, Pgis1, Idd21.1, Lbw6*
18[d]	rs13483466	82,40	3.0	rs3720876-rs13483482	*Cia18*	*Eae25, Idd21.1*

a. Position according to the NCBI Build 37.

b. Significance level determined by ANOVA.

c. QTLs retrieved from MGI database.

(http://www.informatics.jax.org/searches/allele_form.shtml).

d. QTLs controlling more than one phenotype.

All QTLs shown have passed the 0.01 significant threshold by 1,000 permutation test. ** indicates QTLs that have passed the 0.001 threshold. Chr, chromosome; CI, confidential interval; bp, base pair.

4.2 Identification of the *Cia27* QT gene

4.2.1 Gene expression analysis

Fine mapping *Cia27*

Initially, it was shown that *Cia27* was controlling specific antibody response. This fact suggests an involvement of the gene underlying the QTL in the adaptive immune system. Following that assumption, it might be expected that the *Cia27*-gene is expressed in any stage of life of the main cell types of the adaptive immune system such as B and T lymphocytes.

After haplotype block *in silico* analysis, six genes were pointed out as main candidates: *Thrap2, Tbx3, Tbx5, Rbm19, Lhx5* and *Sdsl* (see section 1.2). To further fine map *Cia27*, the expression of the candidate genes was determined in B and T cell populations of the DBA/1J and FVB/N strains.

B cells ($B220^+$) and T cells ($CD3^+$) from spleen from DBA/1J and FVB/N mice were sorted via fluorescence activated cell sorting (FACS). In each strain, two spleens from healthy adult mice were pooled prior sorting. Total RNA was isolated from sorted cells and cDNA was synthesized by reverse transcription. Gene expression was determined by quantitative real-time PCR using TaqMan assays, and data was normalized to *Gadph* expression. *Thrap2* and *Rmb19* were the most expressed genes in B and T cells (Figure 4.2 A) and both showed a higher expression in DBA/1J than in FVB/N. Of the rest, half (*Tbx5* and *Lhx5*) were undetectable and the remainder (*Tbx3* and *Sdsl*) had very low expression (Figure 4.2 B).

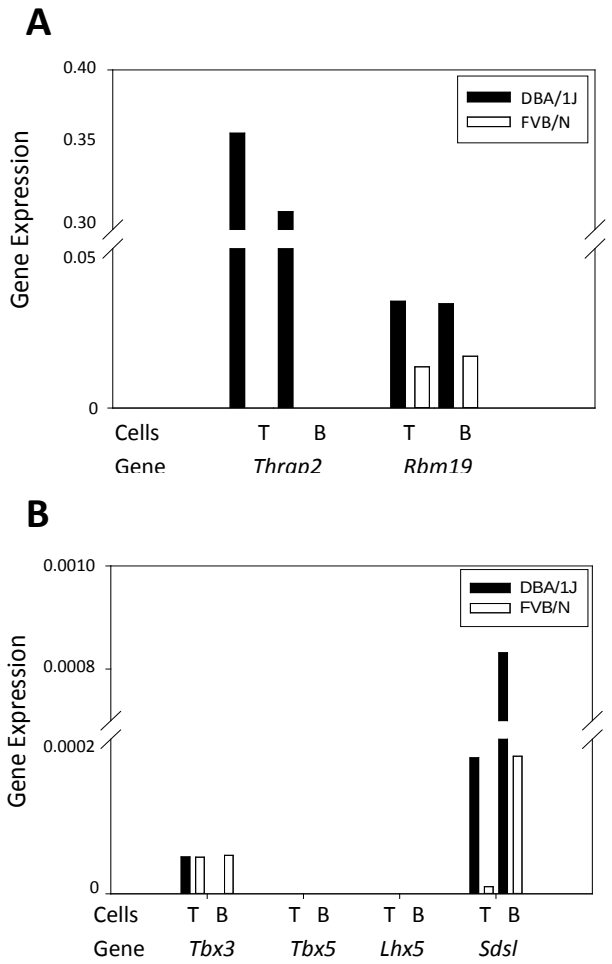

Figure 4.2. Comparative expression profiling of candidate genes. Gene expression levels were assayed in splenic B and T cells from adult healthy DBA/1J and FVB/N mice by real-time PCR. A pool of the spleens from two mice was used per strain and every sample was duplicated. Gene expression was normalized to *Gapdh*. *Thrap2* and *Rmb19* were high expressed in both strains in comparison with the other candidate genes. *Tbx3* and *Sdsl* showed a very low expression in B and T cells from both strains, while *Tbx5* and *Lhx5* were undetectable.

To validate these results, *Thrap2* and *Rbm19* expression was analyzed in splenic B and T cells from three mice of each strain, following the same procedure as above. *Thrap2* and *Rbm19* were significantly upregulated in B cells from DBA/1J mice in comparison with B cells from FVB/N mice (at least 3-fold difference for *Thrap2* and 2-fold difference for *Rmb1*9, $P < 0.02$) (Figure 4.3). No significant differences in the expression of *Thrap2* and *Rbm19* in T cells were found between DBA/1J and FVB/N

mice. Moreover, *Thrap2* expression was more than 2-fold higher than *Rbm19* expression in B and T cells from DBA/1J mice and T cells from FVB/N ($P \leq 0.005$).

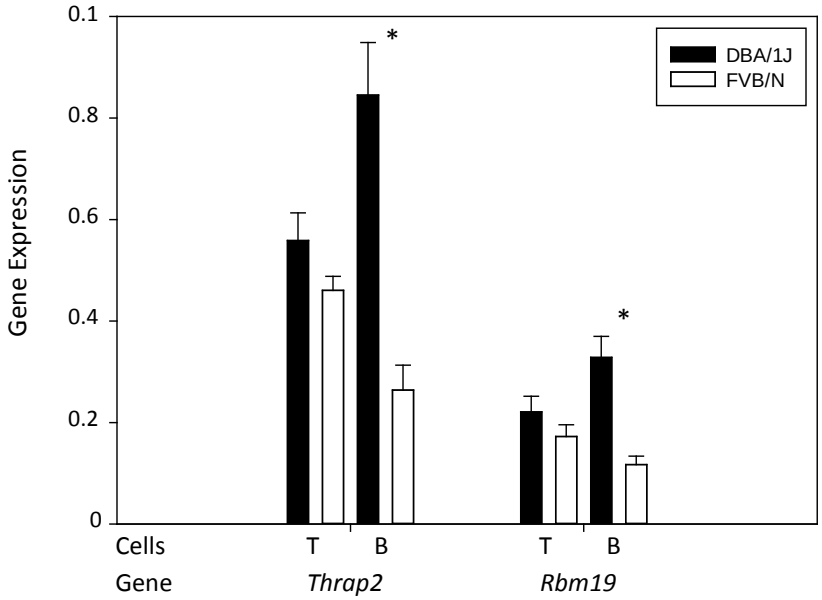

Figure 4.3. Confirmation of expression levels of *Thrap2* and *Rbm19* in splenic B and T lymphocytes. Spleens from three adult healthy mice from each strain were pooled and B and T cells were sorter by FACS. Total RNA was isolated, and *Thrap2* and *Rbm19* expression was determined by real-time PCR in triplicates. One of the FVB/N B samples was excluded as outlier. Gene expression was normalized to *Gapdh*. B cells from DBA/1J mice showed > 3-fold higher expression of *Thrap2* and > 2-fold higher expression of *Rbm19* compared with B cells from FVB/N mice. Each bar represents the mean of three samples and error bars represent standard deviation (SD). For statistical comparison, t-test was used. * $P < 0.02$.

Thrap2 expression in spleenic lymphocytes

Due to the high levels of *Thrap2* transcripts found in splenic B cells and T cells and given the differences in transcript levels between DBA/1J and FVB/N, next experiments focused on *Thrap2*. In order to further investigate the target cell of *Thrap2*, quantitative analysis of mouse spleen compartments during immune reaction was performed. To

prime the immune system, 5 homozygous B10q.C3H subcongenic mice and 5 wildtype B10q mice were intra-peritoneally immunized with alumOVA. At day 10 post-immunization, *Thrap2* expression was determined in the spleen compartments previously microdissected.

The production of *Thrap2* transcripts by B10q.C3H mice was similar to that of B10q mice when comparing the same compartments (Figure 4.4). However, interesting differences were found between compartments. The levels of *Thrap2* transcripts in red pulp were significantly higher than in PALS and follicles (P = 0.008). Similarly, marginal zone *Thrap2* transcript levels were significantly higher than in PALS (P = 0.008) and markedly higher than in follicles (P = 0.56) (Table 4.5).

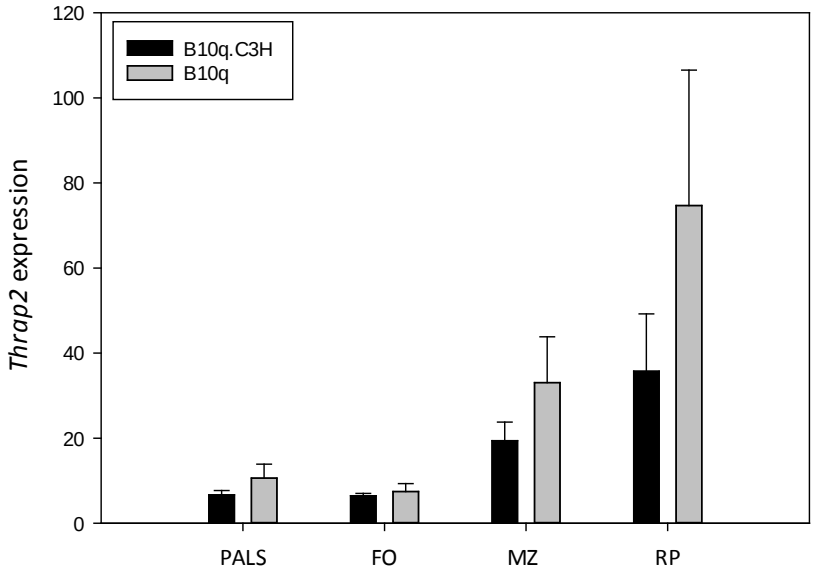

Figure 4.4. *Thrap2* expression levels in splenic compartments. *Thrap2* transcription level was determined in different splenic compartments of 5 B10q.C3H congenic mice and 5 B10q wt mice at day 10 after alumOVA-immunization. Every sample was duplicated and gene expression was normalized to *Mln51*; data from two independent experiments were pooled because they had similar expression levels. *Thrap2* expression was significantly higher in MZ and RP than in PALS or FO in samples from both strains. PALS, periarteriolar lymphatic sheath; MZ, marginal zone; FO, B cells follicles; RP, red pulp.

Table 4.5. Comparison of *Thrap2* expression levels between splenic compartments

Strain	Compartment	*Thrap2* expression	*P* value *vs* RP	*P* value *vs* MZ
B10q	PALS	10.62 ± 3.39	0.008	0.008
	FO	7.46 ± 1.86	0.008	0.056
	MZ	33.75 ± 13.49	0.095	-
	RP	74.69 ± 31.84	-	-
B10q.C3H	PALS	6.70 ± 1.01	0.008	0.011
	FO	6.49 ± 0.54	0.008	0.008
	MZ	19.43 ± 4.35	0.141	-
	RP	35.75 ± 13.49	-	-

Statistics were calculated with ANOVA and Mann–Whitney U test.

PALS, periarteriolar lymphatic sheath; MZ, marginal zone; FO, B cells follicles; RP, red pulp.

4.2.2 *Eae39* subcongenic strains

To further resolve *Cia27* QTL, C19 and C20 subcongenic fragments were tested. Figure 4.1 shows the region included in the C19 and C20 fragments. Borders of both fragments were further refined. *Thrap2* was the only gene contained in the C19 fragment (between markers rs46503071 and rs47812069), and as a consequence, it was the only gene with RIIIS/J alleles in the C19 subcongenic strain. The uncertainty region – defined as the region between the last genotyped allele of the donor strain and the first genotyped allele of the recipient strain in the border of a given congenic fragment – was larger in the C20 fragment, due to the absence of known polymorphism between the RIIIS/J and B10.RIII strains in that region. That fact limited the accurate identification of the genes present in the fragment. The C20 fragment (between rs33221511 and rs46503071) comprises the genes: *Vsig10*, *Wsb2*, *Rfc5*, *Ksr2*, *Nos1*, *Fbxo21*, *Tesc*, *Fbxw8*, *Hrk*, *Rnft2* and *2410131K14Rik*. The informative marker

D5teschm15 maps to *Tesc* gene. This confirms the presence of RIIIS/J alleles at that position.

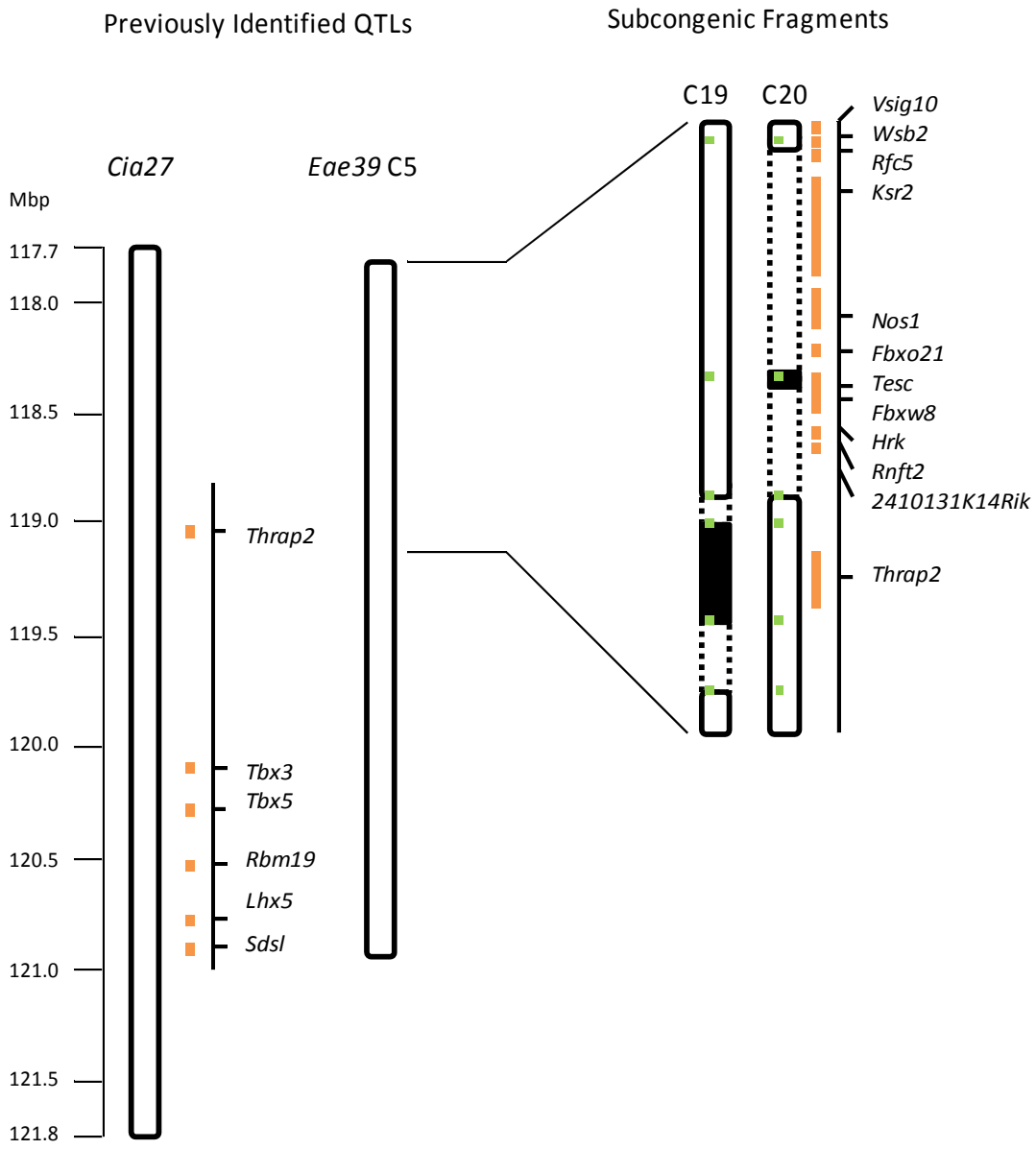

Figure 4.5. *Cia27* and *Eae39* QTLs. Schematic representation of the *Cia27* and *Eae39* QTLs (left) and the C19 and C20 subcongenic fragments (right). The left margin shows the position on chromosome 5. In the subcongenic strains, the chromosomal regions inherited from the RIIIS/J strain are shown in black and the inherited from B10.RIII, in white. Ambiguous regions are

represented with a dotted line; green dots indicate genotyped locations. Candidate genes from the *Cia27* and *Eae39* QTLs are represented in orange.

4.2.2.1 Phenotypic analysis of the C19 and C20 strains

To investigate the effect of RIIIS/J alleles in *Thrap2* gene on disease, the C19 subcongenic strain was tested for CIA development. A set of mice containing C19 homozygous and heterozygous males were immunized with CII; as controls B10.RIII littermate and C20 homozygous and heterozygous males were immunized (Figure 4.6). Susceptibility, maximum score, disease severity (measured as area under the curve (AUC)), and anti-CII IgG2c, IgG1 and total IgG levels at day 21 and 56 were used to phenotype the mice.

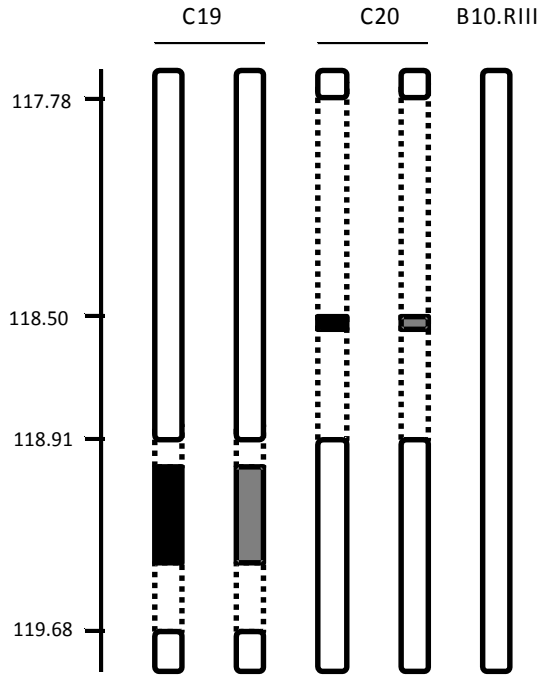

Figure 4.6. *Eae39* C19 and C20 subcongenic strains CIA experiment. Left margin shows the position on chromosome 5. Two B10.RIII alleles are represented in white, two RIIIS/J alleles in black, and heterozygous in grey. Positions according to NCBI release 37 of the mouse genome assembly.

Disease phenotypes

In Figure 4.7, the disease development of the fragments described in Figure 4.6 is shown. Both C20 homozygous and heterozygous fragments developed more severe disease compared with B10.RIII control (Figure 4.7, Table 4.6). C20 heterozygous mice showed higher maximum score (51.5 ± 4.3, $P < 0.05$) and AUC (1,706 ± 111, $P < 0.05$) when compared with the B10.RIII controls (maximum score = 27.7 ± 6.4; AUC = 837 ± 168).

C19 heterozygous fragment showed slightly more severe disease than B10.RIII littermates, although the differences were not significant (maximum score = 44.0 ± 4.2; AUC = 1,150 ± 183). The differences in the disease course of the C19 homozygous fragment resulted even more discrete than in the C19 heterozygous fragment (maximum score = 35.4 ± 3.1; AUC = 964 ± 92). Susceptibility to disease was not affected by the RIIIS/J alleles.

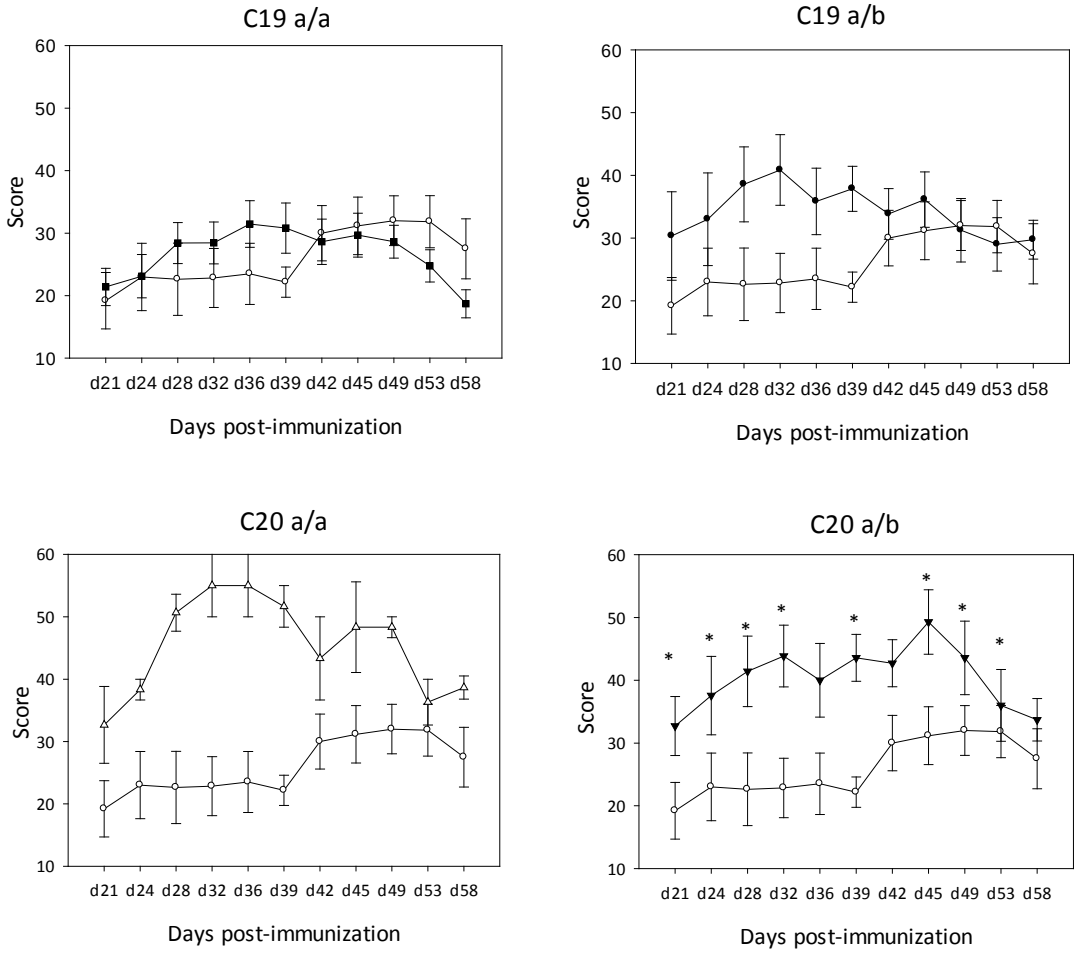

Figure 4.7. CIA progression in *Eae39* C19 and C20 subcongenic strains. Representation of scores (mean ± SEM) of the congenic fragments described in Figure 4.6 *versus* day post-immunization. Statistics were calculated with Mann–Whitney U test. C19 a/a, n = 21, (■); C19 a/b, n = 8, (●); C20 a/a, n = 3, (△); C20 a/b, n = 7, (▼); B10.RIII b/b, n = 10 (○). a = RIIIS/J alleles, b = B10.RIII alleles. * $P < 0.05$.

Table 4.6. CIA disease phenotypes

Congenic Fragments	Alleles[a]	Incidence		Maximum score[b]	AUC[b]
		No.	%		
C19	a/a	21/21	100	35.4 ± 3.1	964 ± 92
	a/b	8/8	100	44.0 ± 4.2	1150 ± 183
C20	a/a	3/3	100	55.0 ± 5	1513 ± 153 *
	a/b	7/7	100	51.5 ± 4.3 *	1706 ± 111 *
B10.RIII	b/b	8/10	80	27.7 ± 6.4	837 ± 168

a. RIIIS/J and B10.RIII alleles in the congenic fragments are symbolized by *a* and *b*, respectively.

b. Mean ± SEM; all immunized mice were included in the calculation.

Statistics were calculated by the Fisher Exact test for susceptibility and by Mann–Whitney U, ANOVA and Kruskal-Wallis test for maximum score and AUC. * $P < 0.05$.

Antibody response

Levels of anti-CII IgG1, IgG2c and total IgG at day 21 and IgG2c and total IgG at day 56 were determined by ELISA and standardized by the 4-parameter curve. A modest increase, though not significant, was observed on IgG1 and total IgG levels at day 21 in subcongenic mice compare with B10.RIII controls (Table 4.7). This trend was also observed on IgG2c and total IgG at day 56 (Table 4.7).

Table 4.7. Anti-CII antibody titers

	C19 a/a	C19 a/b	C20 a/a	C20 a/b	B10.RIII b/b
Day 21					
IgG1	2.253 ± 0.388	1.710 ± 0.355	2.190 ± 1.173	2.219 ± 0.446	1.424 ± 0.505
IgG2c	0.308 ± 0.046	0.335 ± 0.075	0.233 ± 0.043	0.230 ± 0.035	0.312 ± 0.048
TotIgG	0.350 ± 0.034	0.360 ± 0.037	0.545 ± 0.205	0.419 ± 0.031	0.293 ± 0.053
Day 56					
IgG2c	0.531 ± 0.099	0.354 ± 0.046	0.244 ± 0.084	0.344 ± 0.045	0.288 ± 0.051
TotIgG	0.675 ± 0.105	0.505 ± 0.069	0.489 ± 0.108	0.603 ± 0.078	0.422 ± 0.069

Relative concentrations are shown as mean ± SEM. Statistics were calculated with ANOVA.

Lymphocyte populations

To check whether RIIIS/J alleles in *Thrap2* affected the frequency of cells in the spleen of disease animals, spleen from five mice with C19 homozygous fragment and five mice with C20 heterozygous fragment as controls, were analyzed by FACS. Total B cells ($B220^{+}$), MZ B cells ($B220^{+}CD21/35^{hi}CD23^{low}$), FO B cells ($B220+CD21/35^{int}CD23^{hi}$), total T cells ($CD3^{+}$), CD4 T cells ($CD3^{+}CD4^{+}$), CD8 T cells ($CD3^{+}CD8^{+}$) and $CD11^{+}$ cells were determined. No difference was seen in the frequency of the different cell types nor in the CD4:CD8 or MZ:FO ratio (data not shown).

Results obtained in this experiment showed that C20 harbors genes that are involved in CIA development. In addition, the difference on disease development between the heterozygous and homozygous C19 mice suggested that genes in the C20 fragment might have an effect on *Thrap2*. The following experiment was directed to investigate the nature of that effect.

4.2.2.2 Phenotypic analysis of the C19/C20 strain

C19 and C20 homozygous mice were intercrossed to generate a new subcongenic strain, called C19/C20. This new strain contained two heterozygous fragments from the RIIIS/J strain: C19 and C20. A new set of C19/C29, C19, C20 and B10.RIII males were CIA-immunized (Figure 4.8).

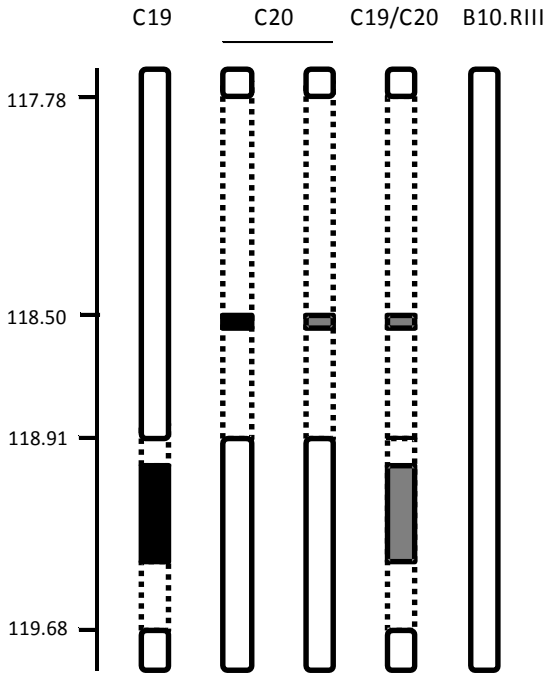

Figure 4.8. *Eae39* C19/C20 subcongenic strains CIA experiment. Left margin shows the position on chromosome 5. Two B10.RIII alleles are represented in white, two RIIIS/J alleles in black, and heterozygous in grey. Positions according to NCBI release 37 of the mouse genome assembly.

Disease phenotypes

Subcongenic mice developed more severe disease compared with controls (Figure 4.9). Interestingly, mice containing the C19 and C20 fragments had a disease pattern similar to mice containing the C20 fragment.

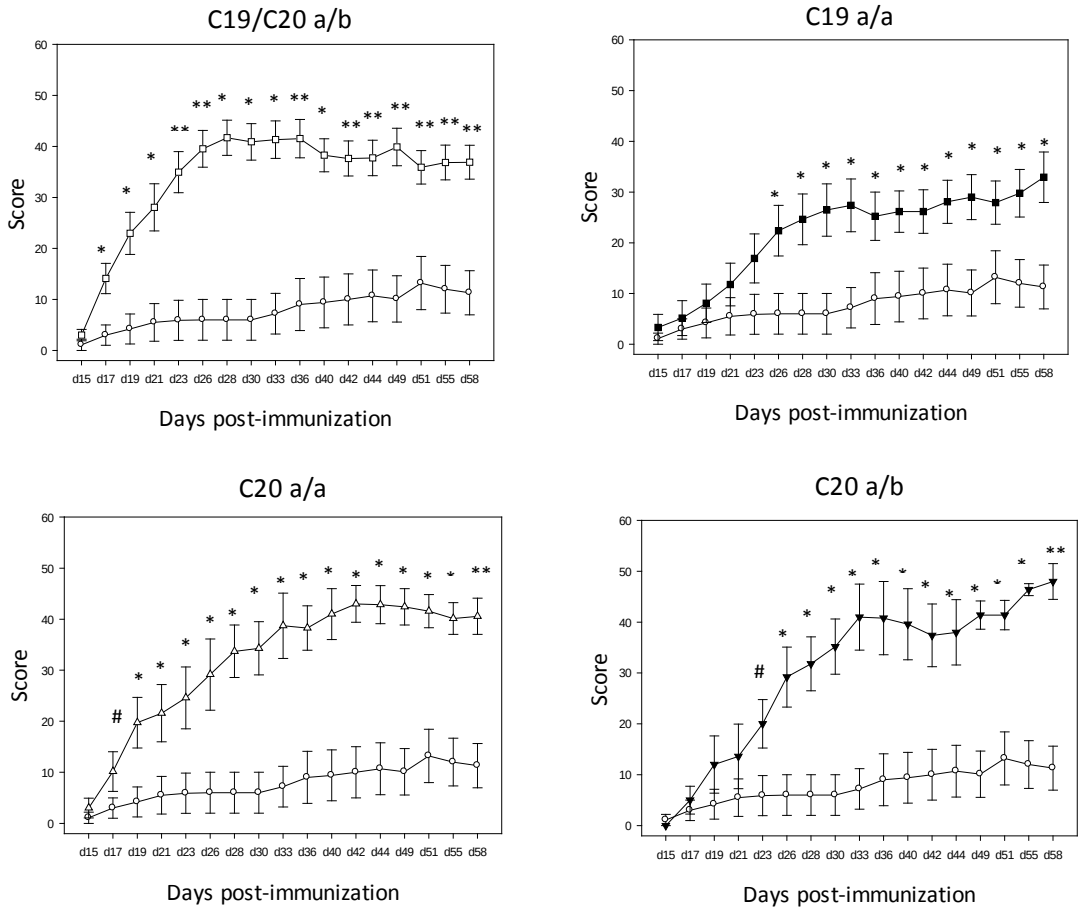

Figure 4.9. Disease development of *Eae39* subcongenic fragments. Representation of the scores (mean ± SEM) of the congenic fragments described in Figure 4.8 *versus* day post-immunization. Statistics were calculated with Mann–Whitney U test or t-Test. A) C19/C20 a/b, n = 19, (□); B) C20 a/a, n = 7, (△); C20 a/b, n = 5, (▼); C) C19 a/a, n = 13, (■); B10.RIII b/b, n = 10, (○). # $P < 0.1$, * $P < 0.05$, ** $P < 0.001$.

In this approach, C19 fragment had higher incidence (100%, $P < 0.01$) and more severe disease (maximum score = 36.3 ± 4.9, $P < 0.01$; AUC = 1,528 ± 132, $P < 0.05$) compared with the B10.RIII controls (incidence = 50%; maximum score = 13.2 ± 5.2; AUC = 355 ± 173) (Table 4.8). In agreement with the previous observations, C19 developed less disease than the C20 fragments and showed significantly lower AUC compared with the C20 homozygous fragment (AUC = 1477 ± 163, $P < 0.05$) (Table 4.8). Furthermore, C19/C20 fragment showed a similar maximum score (49.1 ± 3.3) and AUC

(1528 ± 132) to C20 fragment (maximum score: a/a = 46.1 ± 4.8, a/b = 50.8 ± 2.7; AUC: a/a = 1,477 ± 163, a/b = 1,431 ± 151). Disease severity in the C19/C20 subcongenic strain was enhanced in comparison with the C19 subcongenic strain ($P < 0.05$). In all the subcongenic strains, onset was not affected by the RIIIS/J alleles.

Table 4.8. CIA disease phenotypes

Congenic Fragments	Alleles[a]	Incidence No.	%	Onset[b]	Maximum score[c]	AUC[c]
C19/C20	a/b	19/19	100 **	19 ± 2	49.1 ± 3.3 **	1528 ± 132 *
C19	a/a	12/13	92.3 **	24 ± 3	36.3 ± 4.9 **	1005 ± 171 *
C20	a/a	7/7	100 **	18 ± 2	46.1 ± 4.8 **	1477 ± 163 *
	a/b	5/5	100 *	19 ± 1	50.8 ± 2.7 **	1431 ± 151 *
B10.RIII	b/b	5/10	50	30 ± 6	13.2 ± 5.2	355 ± 173

a. RIIIS/J and B10.RIII alleles in the congenic fragments are symbolized by *a* and *b*, respectively.

b. Onset measured in days. Mean ± SEM; only disease mice were included in the calculation.

c. Mean ± SEM; all immunized mice were included in the calculation.

Statistics were calculated by the Fisher Exact test for susceptibility and by Mann–Whitney U, ANOVA and Kruskal-Wallis test for maximum score and AUC. ** $P < 0.01$ * $P < 0.05$.

Antibody response

Anti-CII antibody levels are shown in Table 4.9. IgG1 and IgG2c titers were increased in the C19/C20, C20 a/a and C20 a/b fragments at day 21 in comparison with B10.RIII controls ($P < 0.05$). Total IgG titers were higher in all the congenic fragment at day 21 compared with the B10.RIII controls ($P < 0.05$). At day 56, IgG1 levels were higher in the C19/C20 and C20 homozygous fragments ($P < 0.05$) and showed a slight increase in the C19 fragment ($P < 0.1$).

Table 4.9. Anti-CII antibody titers

	C19/C20 a/b	C19 a/a	C20 a/a	C20 a/b	B10.RIII b/b
Day 21					
IgG1	1.323 ± 0.357*	0.796 ± 0.246	0.932 ± 0.173*	2.175 ± 1.124*	0.292 ± 0.160
IgG2c	0.158 ± 0.020*	0.138 ± 0.041	0.129 ± 0.011*	0.162 ± 0.029*	0.076 ± 0.018
TotIgG	0.231 ± 0.026*	0.223 ± 0.065*	0.211 ± 0.035*	0.247 ± 0.060*	0.080 ± 0.026
Day 56					
IgG1	2.285 ± 0.504*	1.949 ± 0.426#	3.229 ± 0.647*	1.196 ± 0.274	1.289 ± 0.650
IgG2c	0.494 ± 0.056	0.472 ± 0.070	0.426 ± 0.0479	0.467 ± 0.075	0.351 ± 0.069
TotIgG	0.685 ± 0.082	0.620 ± 0.122	0.862 ± 0.162#	0.400 ± 0.052	0.459 ± 0.110

Relative concentrations are shown as mean ± SEM. Statistics were calculated with ANOVA and Kruskal–Wallis one-way analysis of variance. * $P < 0.05$, # $P < 0.1$.

4.2.2.3 *In vitro* experiments

To investigate the function of *Thrap2*, knockdown assays were performed in murine B cells and T cells using small-interfering RNAs (siRNA). *Thrap2* was specifically inhibited by Accell SMARTpool siRNA targeting *Thrap2* (Thrap2 siRNA). Cells treated with Accell Non-targeting siRNA were used as control.

B cells isolated from mouse spleen (SP B cells) were transfected with Thrap2 siRNA or Non-targeting siRNA and cultured in medium alone or in the presence of LPS (50 µg/ml), LPS + anti-Ig (50 µg/ml and 2 µg/ml, respectively) or anti-CD40 (10 µg/ml). siRNA treatment was performed 16 h prior to stimulation. Cells were analyzed by FACS at three different time points (8 h, 1 day and 3 days) after the stimulation. Non-stimulated cells treated with Thrap2 siRNA displayed a significant increase in viability (*P*

< 0.01) with a reduction in specific cell death after 8 h and 1 day in comparison with Non-targeting siRNA treated cells (Figure 4.10 A). A similar effect was also observed in cells cultured with different stimuli at 8 h and 1 day post-stimulation and Thrap2 siRNA treated cells showed a decrease in specific cell death compared with control (Figure 4.10 A).

The level of cell activation was determined by the presence of activation markers (CD69 and CD25) and plasma cell ($CD138^{+}$) (Figure 4.10 B). Cells transfected with Thrap2 siRNA showed a slight increase in cell activation 8 h and 1 day post-stimulation compared with Non-targeting siRNA treated cells (Figure 4.10 B). At day 3, most of the cells were dead (data not shown).

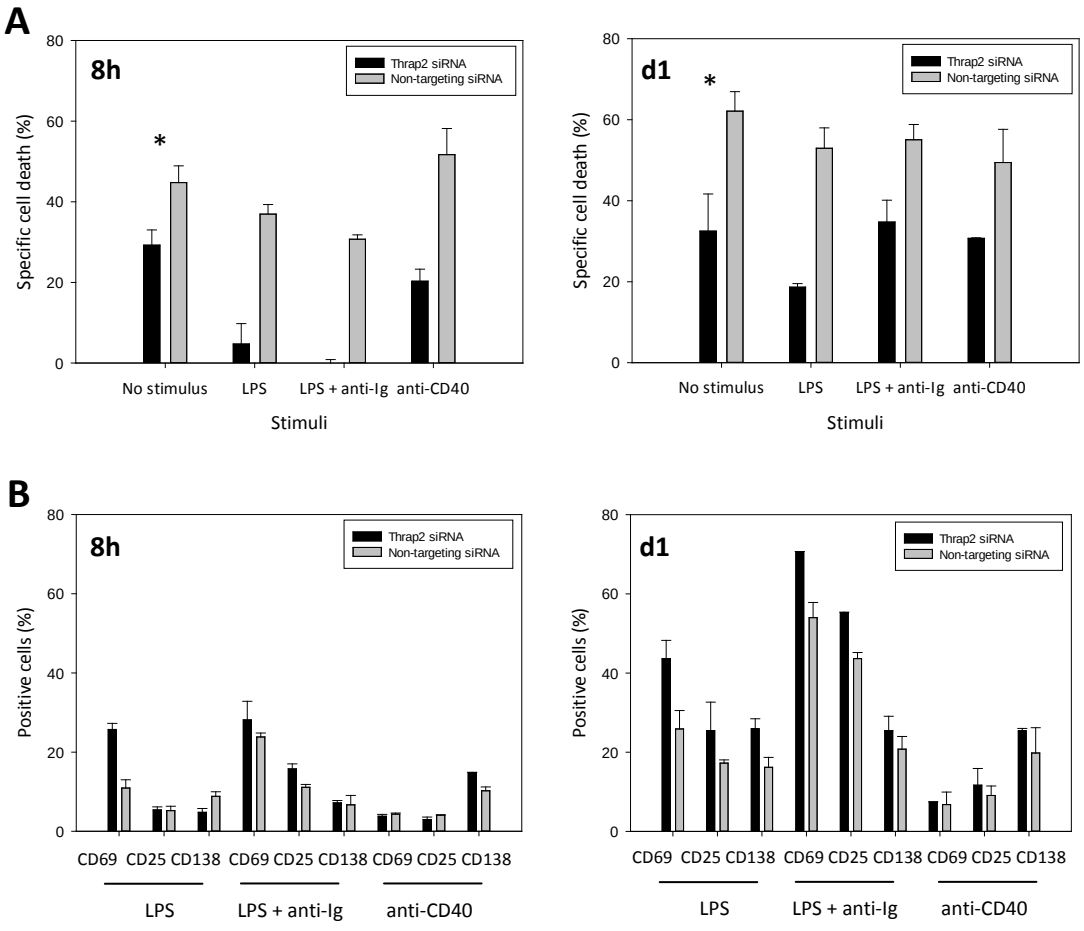

Figure 4.10. *Thrap2* knockdown assay in B cells cultures. Primary murine splenic B cells were cultured in presence of Thrap2 siRNA or Non-targeting siRNA. Sixteen h post-transfection cells were stimulated with LPS, LPS + anti-Ig or anti-CD40 for 3 days. One group of cells was not stimulated. Cells were analyzed by FACS at different time points. (**A**) Specific cell death was evaluated with 7-AAD at 8 h and 1 day after stimulation. (**B**) Percentage of cells expressing CD69, CD25 and CD138 were determined at 8 h and 1 day after stimulation. Experiments were performed in triplicates for the non-stimulated cells and in duplicates for the rest. Bars represent mean ± SD. Statistical analysis was performed by t-test. * $P < 0.01$.

In section 4.2.1, it was shown that *Thrap2* was highly expressed in MZ and RP. To investigate whether the effect of *Thrap2* upon B cells will be observed in other B cells subsets, lymph nodes (LN) B cells were tested as well as SP B cells.

In the previous knockdown experiment almost no cells were alive at day 3 after stimulation. In order to improve general cell survival, minor modifications in the culture conditions were included: LPS concentration was decreased to 10 µg/ml, LPS was incorporated in the culture 8 h after siRNA incubation instead of 16 h, and 100 µl of extra fresh media was added to the culture at stimulation. In addition, to test whether cell viability could be improved with the elimination of the siRNA incubation time prior stimulation, a set of SP B cells were transfected and stimulated simultaneously. Cell viability was not altered regardless the stimulation time point.

As expected SP B cells treated with Thrap2 siRNA showed a significant reduction ($P < 0.05$) in specific cell death compared with controls (Figure 4.11). In contrast, difference in cell viability was not observed between LN B cells incubated with Thrap2 siRNA and controls.

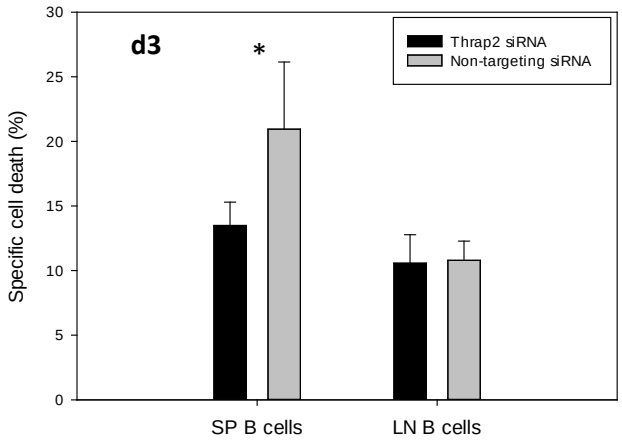

Figure 4.11. *Thrap2* knockdown assay in B cells from spleen and lymph nodes. Primary mouse spleen (SP) and lymph nodes (LN) B cells were cultured in presence of SMARTpool Thrap2 siRNA or Non-targeting siRNA. LN B cells were stimulated with LPS at 8 h post-transfection. SP B cells were stimulated with LPS at 8 h post-transfection or simultaneously at transfection. Since differences were not found between both protocols of stimulation, data were analyzed together. At day 3 post-stimulation, specific cell death was evaluated with DAPI by FACS. Experiments were performed in duplicates. Bars represent mean ± SD. Statistical analysis was performed by t-test. * $P < 0.05$.

Thrap2 knockdown assay was also carried on CD4 T cells. CD4 T cells isolated from mouse spleens were cultured in presence of Thrap2 siRNA or Non-targeting siRNA. After 16 h, cells were stimulated with anti-CD3 (5 µg/ml) and anti-CD28 (2 µg/ml). Cell viability and activation was analyzed by FACS at 8 h and 1 day after stimulation. No differences in viability (Figure 4.12 A) or cell activation (Figure 4.12 B) were found either at 8 h or 1 day post-transfection (Figure 4.12 A and B).

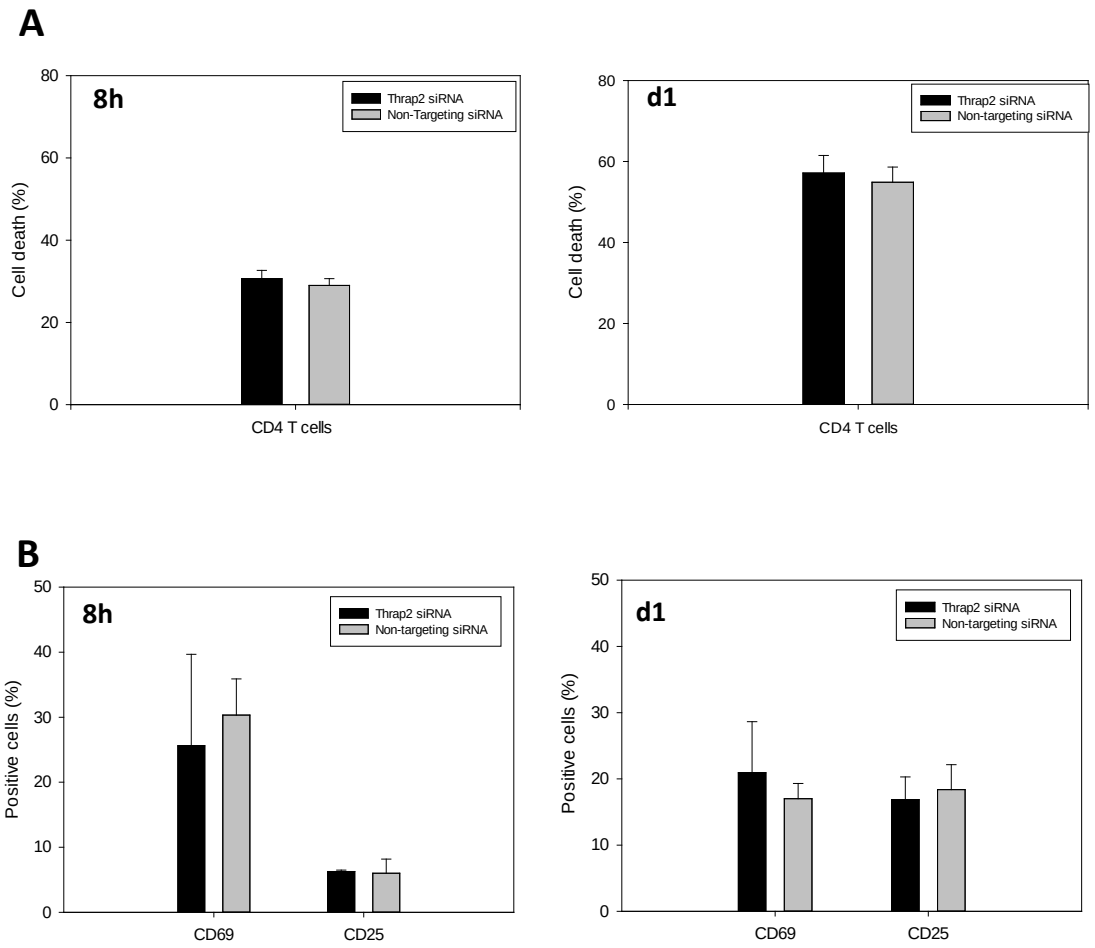

Figure 4.12. *Thrap2* knockdown assay in CD4 T cell from spleens. Primary murine splenic CD4 T cells were cultured in the presence of *Thrap2* siRNA or Non-targeting siRNA. Sixteen h post-transfection, cells were stimulated with anti-CD3 and anti-CD28. Cells were analyzed by FACS at different time points. (**A**) Percentage of cell death was evaluated with 7-AAD at 8 h and 1 day after stimulation. (**B**) Percentage of cells expressing CD69 and CD25 was determined 8 h and 1 day after stimulation. Statistical analysis was performed by t-test.

4.2.3 Human association study

Ultimately, a case-control association study in an Egyptian population was conducted. Three SNPs mapped in the human chromosomal region syntenic to *Cia27* were tested as candidate SNPs. These SNPs were previously reported to be associated with RA or

Type I diabetes (T1D) in European or American with European ancestry populations (Table 4.10).

Genotyping results are summarized in Table 4.11. None of the studied SNPs achieved statistical significance for association with rheumatoid arthritis risk (Table 4.12). Population stratification by gender and presence of autoantibodies was also analyzed, and no statistical effect of these 2 parameters was observed (data not shown).

Table 4.10. Known SNPs associated with RA and T1D in the corresponding human locus

SNP ID	Position (bp)[a]	Type	Closest gene/s	Population	Disease
rs10507251	114987794	Intergenic	*TBX3* and *TBX5*	American[b] and Spanish	RA [80]
rs17580303	116539384	Intronic	*MED13L*/*THRAP2*	British	TD1 [81]
rs9788041	118473054	Exonic	*WSB2*	British	RA [81]

a. Coordinates are given relative to NCBI build 37.3 of the human genome assembly.

b. Brigham Rheumatoid Arthritis Sequential Study (BRASS) cohort, American with European Ancestry.

Table 4.11. Summary of genotype results

SNP	Allele	Control	Cases
rs10507251	**CC**	0	1
	CG	20	15
	GG	334	298
	Total	*354*	*314*
rs17580303	**CC**	1	3
	CG	31	34
	GG	315	270
	Total	*347*	*307*
rs9788041	**CC**	31	36
	CT	138	113
	TT	187	113
	Total	*356*	*318*

Table 4.12. Statistical analysis

SNP	MA	MAF	*P* value[a]
rs10507251	C	0.027	*0.503*
rs17580303	C	0.027	*0.339*
rs9788041	C	0.291	*0.441*

a. Statistical analysis was performed by χ^2 test.

MA, minor allele; MAF, minor allele frequency in control group.

5 Discussion

RA is a common disorder mediated by multiple underlying genes [82]. Strong evidence supports that RA is rather a syndrome than a discrete disease with a single etiologic source [83, 84]. In fact, RA has already been divided according to the presence or absence of ACPA [85]. This division is also reflected in the genetic heterogeneity and clinical phenotype: HLA-DRB1 and PTPN22 loci are exclusively associated with ACPA-positive patients who, in addition show more severe and destructive disease than ACPA-negative patients [86, 87]. However, it is likely that there are more than two subsets of RA. Further evidence supporting this notion are the heterogeneity of clinical phenotypes between individuals and the ethnic heterogeneity in risk loci associated to RA. Regarding the first one, RA patients present a broad diversity of clinical symptoms, mainly at early stages of disease, which brings about the necessity of large range of criteria (see Table 1.1) to define and diagnose the disease. This heterogeneity is likely to be one of the causes of the limitation of GWAS to identify and replicate loci underlying RA [88]. Other causes may be the effect of structural and rare variants, poorly covered in GWAS. A good example for the ethnic heterogeneity, is the *PTPN22* gene, which is the second largest RA genetic risk factor in populations of European descent; however, it has not been associated in Asiatic population, where the second most important genetic risk is *PADI4* [89].

It is apparent the need to study RA from various perspectives to gain more insight into the several pathogenic mechanism which could lead to RA in different individuals. Animal models are excellent tools for this purpose. The different animal models of RA most likely mimic different pathways implicated in arthritis and may therefore be controlled by specific set of genes. It is noteworthy that, due to its genetic feature, a disease in a given inbred strain is likely to represent disease in one single or in related human individual rather than in a heterogeneous population. Thus, it may be

convenient to use more than one animal strain to better reflect the complexity of the human disease.

In the first part of this study, the most extensive genetic analysis of BXD2/TyJ spontaneous arthritis was generated. Twenty-one arthritis loci were identified of which 6 had not been implicated in any previous genetic studies in arthritis. Although no QTL was fine-mapped in sufficient detail to identify the causal genetic variant, potential candidate genes of certain QTLs are highlighted below.

One of the most strongly associated loci maps towards the telomeric end of chromosome 18 and controls susceptibility, maximum score and onset of disease. This locus spans the previously identified *Pgia11* and *Cia18* loci, which are associated with susceptibility to arthritis and autoantibody production, respectively [65, 90]. This locus also overlaps with loci associated with the murine models of multiple sclerosis (*Eae25*) [91], systemic lupus erythematosus (*Lbw6*) [92], T1D (*Idd21.1*) and autoimmune ankylosing spondylitis (*Pgis1*) [93]. The importance of chromosome 18 in susceptibility to autoimmunity in different species had already been reported [94]. In fact, the QTL identified in this study contains genes which human orthologous have been associated with RA in a GWAS study [81] such as *PTPN2* (protein tyrosine phosphatase, non-receptor type 2, lymphoid), *TCF4* (transcription factor 4), *ZBTB7C* (zinc finger and BTB domain containing 7C), *IMPA2* (inositol(myo)-1(or 4)-monophosphatase 2), *CBE1* (collagen and calcium binding EGF domains 1), *ALPK2* (alpha-kinase 2), *ATP9B* (ATPase class II type 9B or macrophage MHC receptor 1), *DYM* (dymeclin), *CTIF* (CBP80/20-dependent translation initiation factor), and *CCDC11* (coiled-coil domain containing 11). Other candidate genes of particular interest within the locus are *Nfatc1* gene encoding calcineurin-dependent nuclear factor 1 of activated T cells; *Smad2*, *Smad7* and *Smad4* genes encoding proteins from the SMAD (similar to mothers against decapentaplegic) family which mediates TGF-β signaling; *Dcc* gene encoding a netrin 1 receptor, a member of the immunoglobulin superfamily of cell adhesion molecules; and *Malt1* gene encoding a caspase-like protein involved in B cell- and T- cell receptor signaling pathways.

On chromosome 19, a locus strongly associated with maximum score and susceptibility was found. This locus overlaps with *Paam2*, a known QTL for susceptibility to spontaneous arthritis [73], which leads to the assumption that this locus harbors critical genes for the development of arthritis in spontaneous mouse models. This QTL has also conservation of synteny with a human region containing genes associated with arthritis [81] such as *ABLIM1* (actin-binding double-zinc-finger protein), *ATRNL1* (attractin-like 1), *XPNPEP1* (X-prolyl aminopeptidase 1), *HABP2* (hyaluronan binding protein 2), *SORCS3* (sortilin-related VPS10 domain containing receptor 3) and *C10orf82* (chromosome 10 open reading frame 82). A more compelling candidate gene is *Tcf7l2* or T cell-specific transcription factor 4 gene.

Chromosome X was associated with susceptibility to disease. This association explains at least part of the strong sex effect on arthritis susceptibility. Accordingly, the phenotypes onset and maximum score, for which no sex effect was found, did not show association with this locus. The region matches with the previously mapped genetic locus *Pgia24* controlling antibody response [90]. Plausible biological candidates are *Ikbkg* gene encoding the NF-κB essential modulator, NEMO, which regulates the activation of NF-κB; *Irak1* gene encoding the interleukin-1 receptor-associated kinase 1; and *Canx* gene encoding calnexin which plays a putative role in antigen presenting pathways.

It is noteworthy that the mouse *Ptpn22* gene (the second strongest risk factor linked to human RA) and the homologous region of the validated RA risk locus CD2/CD58 [95] map on chromosome 3 on a locus associated with susceptibility in this cross. In addition, the mouse counterpart of the human arthritis associated *Stat4*, *Cd28* [95] and *Ctla4* [96] loci are harbored on chromosome 1; *Stat4* is included on one locus associated with susceptibility, while *Cd28* and *Ctla4* loci are associated with the three phenotypes. These are gene-rich regions and further studies are required to validate the causality of these genes. However, the fact that 5 human loci had corresponding loci in this cross indicates that it is likely that there are important common genes and pathways involved in arthritis in both humans and animals, particularly in the BXD2/TyJ strain. This is robust evidence supporting that the approach followed in this study is

appropriate and powerful to study genetic factor determining human RA in a hypothesis-free manner. This is even more remarkable if one takes into account the limitations of the study: in genetic association analysis, contributions to disease can only be detected when the polymorphic alleles segregate in the studied population. The relatively low level of recombination of the G4 already allows the identification of human validated loci in mice. This indicates that an increase in the number of generations in the AIL possibly would not only refine the location of the identified QTLs, but also provide more relevant information about the genetic factor of disease.

In summary, the present study demonstrates the utility of the generated four-way autoimmune-prone AIL to identify QTL affecting arthritis. Here, there are successfully identified 6 QTLs strongly associated and 15 QTLs associated with clinical arthritis. This study confirms QTLs previously found in other arthritis models and identifies new risk loci for experimental arthritis. Further, fine mapping within each QTL combined with functional studies will be required to identify the causal genes and the pathways leading to disease.

The second aim of this thesis was to identify the causative gene governing the *Cia27* quantitative trait and to inquire into its contribution to disease applying classical mouse genomic methods such as gene expression analysis, subcongenic strains, *in vitro* functional studies and homology analysis. Fine mapping studies previously performed in our group (see introduction 1.3) identified six candidate genes in the *Cia27* locus. These genes represented the starting point for the following gene identification studies.

Often, the identification of the relevant gene underlying a QTL goes through the elimination of possibilities that are unpromising [97]. It is reasonable to speculate that genes which are not expressed in key cell subtypes or tissues are not actively involved in disease. Equally, those genes that do not present any polymorphism between the strains used to detect the QTL are unlikely to be responsible for the trait. From the initial six candidate genes, four were not or only expressed at low level in isolated splenic T cells and B cells from healthy mice (Figure 4.2). These results were consistent with a previous test performed by our group in total lymph nodes (data not published), and were confirmed by the Immunological Genome Project (ImmGen). According to

ImmGen database, *Tbx3, Tbx5, Lhx5* and *Sdsl* genes present considerably low expression values (< 110) in key population from the immune system, including several subclasses from B cells, T cells, natural killers, monocytes, macrophages, dendritic cells (DCs) and neutrophils; whereas *Thrap2* and *Rbm19* expression values in the same populations range between 300 to 900 and 100 to 250, respectively.

A further study demonstrated that *Thrap2* transcript levels were 3-fold higher in splenic B cells from healthy arthritis-prone mice than in arthritis-resistant mice ($P < 0.02$). Similar results were obtained for *Rbm19* but with lower levels (2-fold higher, $P < 0.02$) (Figure 4.3). When comparing the expression values of both genes, *Thrap2* expression was shown to be 2-fold upregulated compared with *Rmb19*, in the same cell population ($P \leq 0.005$). Taking together these results pointed to *Thrap2* and *Rbm19* genes as main candidate genes.

Although RA has many features of autoimmunity, non-immunologic factors also play a prominent role in disease [98, 99]. To rule out the possibility that differential expression of the *Cia27* QT gene in synoviocytes or synovial tissues was the cause of the *Cia27* phenotype, expression level of five candidate genes (*Rmb19*, *Tbx3, Tbx5, Lhx5* and *Sdsl*) before immunization and at different phases of CIA (10, 35 and 95 days after immunization) were compared between DBA/1J and FVB/N mice (data not published). Except *Tbx5*, none of the genes showed a strain-specific differential expression. *Tbx5* showed differential expression ($P < 0.05$) between DBA/1 and FVB/N in healthy joints before immunization (data not published). Thus, these results suggest that during CIA development differences in the expression of these genes in joints do not control *Cia27* quantitative trait. Whether differential expression of *Tbx5* in joints of naïve mice is relevant for disease development, could not be fully discarded.

As mentioned above, presence of polymorphism is evidence that supports the link of a given gene with a QTL. In this regard, three structural polymorphisms in the proteins coded by *Thrap2* and *Tbx3* genes were previously identified between the parental strains used to identify *Cia27* (see section 1.3). When combining these findings with the gene expression data, *Thrap2* emerged as the strong favorite gene underlying *Cia27* since it shows appropriate characteristics that could explain the trait: i) high

expression in relevant cell-types, at least in comparison with the other candidate genes, ii) strain-specific differential expression, and iii) structural changes in the protein amino acid sequence. Thus, we hypothesized that *Thrap2* was underlying *Cia27* phenotype. Further analysis aimed to confirm this hypothesis and to decipher how *Thrap2* could affect disease.

When analyzing the different splenic compartments of congenic and wildtype strains along alumOVA immunization, no differences were found in the expression levels of *Thrap2* between both strains (Figure 4.4). However, clear upregulation of *Thrap2* in red pulp and marginal zone compared with T cell zone and follicles was detected (Table 4.5). Concerning leukocyte populations, red pulp hosts mainly plasmablasts and plasma cells, and in a lower number DCs and macrophages. Marginal zone main resident cells are MZ B cells, MZ macrophages and MZ metallophilic macrophages, and temporary T cells, B cells and DCs from the bloodstream that enter the white pulp [100]. These observations might indicate that MZ B cells and plasma cells could be the main B cell subtypes responsible for *Thrap2* expression.

Eae39 QTL was identified in a cross between the B10.RIII and RIIIS/J strains as a locus controlling experimental autoimmune encephalomyelitis (EAE) severity [101]. *Eae39* locus overlapped with *Cia27* locus, and subsequently *Eae39* was linked to CIA severity and specific antibody production [64]. Since both *Cia27* and *Eae39* QTLs map in the same genomic region and control similar traits, we assumed that the same gene was underlying both QTLs. In addition, two *Thrap2* polymorphisms (rs13478486 and rs33215085) identified in the DBA/1J and FVB/N strains are also polymorphic between the B10.RIII and RIIIS/J strains. Therefore, the *Eae39*-subcongenic strains were considered appropriated to accomplish the objectives of this work.

It is well-known that QTLs responsible for complex traits can consist of more than one QT gene that act in similar or opposite direction [64, 102, 103]. Thus, to subdivide the locus in subinterval loci is a common method to identify the real contribution of each locus to disease and to reduce the number of possible causative genes. The C19 and C20 subcongenic strains carry RIIIS/J alleles in the congenic loci (see Figure 4.5) and are derived from the original *Eae39* locus. By consecutive breeding, the

Eae39 locus was dissected in several subinterval loci with opposite contributions [64]. One subinterval locus, C5 (112.5 - 120.6 Mbp), was in turn dissected into smaller subinterval loci such as C19 (118.9 - 119.6 Mbp) and C20 (117.7 - 118.9 Mbp). In the present study, to provide evidence of the role of *Thrap2* in CIA, the C19 subcongenic strain was used. To determine whether genes located upstream of *Thrap2* were also involved in CIA, the C20 subcongenic strain was also tested.

In the first study, mice carrying RIIIS/J alleles in the C19 locus showed no significant differences in susceptibility, severity (Table 4.6) or antibody titers (Table 4.7) to control mice, though an increase in antibody response was observed in C19 mice. This was probably due to the extremely high susceptibility and severity of disease that affected B10.RIII control mice in this study. B10.RIII showed an incidence of 98%, a percentage unusually high for this strain which normal susceptibility to CIA is close to 50% [64], as it was shown in the second study. In concordance with this, AUC and maximum score of B10.RIII control mice were significantly higher in the first study than in the second ($P < 0.01$).

It is noteworthy that in the second study mice carrying two alleles of the RIIIS/J strain in the C19 fragment showed higher susceptibility ($P < 0.01$) and developed more severe disease ($P < 0.05$) than B10.RIII controls (Table 4.8). In addition, total specific antibody titers were significantly increased at day 21 in C19 mice compared with controls ($P < 0.05$). These findings correlate with the *Cia27* phenotype. Furthermore, in the previous F2 and AIL studies, DBA1/J alleles in *Cia27* locus were linked to an enhancement of antibody production and disease severity (data not shown). RIIIS/J and DBA1/J share identical alleles in two of the three non-synonymous polymorphisms held on *Thrap2*, and in agreement with this, here it is shown that RIIIS/J alleles in *Thrap2* had a phenotype of higher antibody production and disease severity. Thus, *Thrap2* non-synonymous polymorphisms are associated with specific antibody response and severity of disease.

Regarding the C20 subcongenic mice, both studies showed that the presence of one or two RIIIS/J alleles in the C20 fragment equally enhanced disease susceptibility and severity of disease in CIA (Table 4.6 and 4.8). Furthermore, in the second

experiment, specific antibody levels were also affected by RIIIS/J alleles, mainly at day 21 (Table 4.9). This increase of antibody production was not significant in the first study, probably due to the extreme response of B10.RIII to the immunization, as noted above. Interestingly, C19/C20 congenic mice produced by intercrossing C19 and C20 homozygous mice, responded to CIA immunization as C20 mice (Table 4.8 and 4.9), suggesting a stronger contribution to disease of the C20 than the C19 locus.

Taken together, these observations show that the *Cia27* QTL harbors at least two genes working in an additive fashion: *Thrap2* (119.01 - 119.21 Mbp) and one gene comprised in the upper region of the QTL (117.78 - 118.90 Mbp). RIIIS/J alleles in these loci increased susceptibility, disease severity and antibody production. In addition, these results suggest that genes contained in the upper region have a stronger effect than *Thrap2*.

Thrap2, also known as *Med13l*, was identified by Muncke et al. in 2003 as gene encoding a novel transcription factor (TF) associated with transposition of the great arteries in humans [104]. *Thrap2* gene is ubiquitously expressed in human and mouse, with highest expression in human skeletal muscle and mouse heart [105]. Thrap2 TF belongs to the Mediator complex subunit 13 family and is a component of the mediator complex [106]. The multiprotein Mediator complex is highly conserved from yeast to mammals and supports initiation and regulation of the enzyme RNA polymerase II (RNAPII). RNAPII accomplishes the transcription of all protein-coding genes and thus requires the general initiation factors (TFIIB, TFIID, TFIIE, TFIIF and TFIIH) and the already mentioned Mediator complex. Mediator operates as an adaptor that supports the assembly of the RNAPII preinitiation complex and controls the RNAPII activity during transcription initiation and elongation [107]. Mediator can bind directly to RNAPII, to the general initiation factors and to the activation domains of many DNA binding transcription factors [107]. Mammalian Mediator is composed of 30 subunits which are organized in four modules: the head, the middle and the tail modules, which form the core module, and the kinase module. Thrap2 is believed to be located in the kinase module [108]. Several lines of evidence suggest that the kinase module is a versatile regulator capable of either repressing or activating transcription. The main member of

the kinase module, Cdk8, is reported to support between others the activation of transcription of several p53 target genes and serum response genes in human cells [107].

Identification of the molecular basis of the C20 locus will probably add further mechanistic insight into the regulation of the antibody production and disease severity in arthritis. The C20 locus potentially harbors 11 genes *Vsig10* (V-set and immunoglobulin domain containing 10), *Wsb2* (WD repeat and SOCS box containing 2), *Rfc5* (replication factor C (activator 1) 5), *Ksr2* (kinase suppressor of ras 2), *Nos1* (nitric oxide synthase 1), *Fbxo21* (F-box protein 21), *Tesc* (Tescalcin), *Fbxw8* (F-box and WD repeat domain containing 8), *Hrk* (harakiri, BCL2 interacting protein), *Rnft2* (ring finger protein, transmembrane 2) and *2410131K14Rik* (RIKEN cDNA 2410131K14 gene). The functional effect of the causative gene can depend either on functional polymorphisms or on differential expression of mRNA. To address the second possibility, the level of expression of the C20 candidate genes were studied in joints and LN from DBA1/J and FVB/N mice at different time points after immunization. Interestingly, three genes were differentially expressed ($P < 0.05$) between both strains in different tissues at different time points: *Wsb2* in joints, LN and thymus at day 0, *Nos1* in joints at day 0, and *Tesc* in joints at day 0 and at day 35 (data not published).

Since *Thrap2* and the causative gene of the C20 locus are mapped very closely in the genome and are controlling the same complex traits, we hypothesized that they are involved in the same pathway. To explore potential molecular interactions between the C20 candidate genes and *Thrap2*, network analyses were performed using Ingenuity software. This software provides networks and interrelated biological processes based on known interactions in the literature. Interestingly, a network linking *Fbxw8* and *Wsb2* to *Thrap2* was identified with p53 as focus molecule (Figure 5.1). P53 was inversely correlated with *Thrap2*: presence of p53 significantly decreased *Thrap2* mRNA levels in a human carcinogen cell line [109].

Conserved pathways are contributing to similar phenotypes in different species. To improve resolution of the C20 locus further to the level of individual genes, the association of the human counterpart genes with RA or other autoimmune diseases was

studied. Three polymorphisms were found to be associated with RA: rs6490130 (*P* = 0.0001) and rs6490131 (*P* = 0.0001) in *KSR2*, and rs9788041 (*P* = 0.00033) in *WSB2* [81]. One of them, rs6490130, was also associated with T1D in the same study (*P* = 1.18e-05). Moreover, rs11068218 (*P* = 0.00065) in *HRK* was associated with T1D [81]. These human data support the linkage of the C20 locus with RA, and lead to the assumption that more than one gene contained in the C20 locus could be relevant for arthritis development. Taking together, *Ksr2*, *Wsb2*, *Hrk* and *Fbxw8* are pinpointed as putative underlying genes of the C20 locus.

It is possible that gene/s in the downstream of the original *Cia27* interval contribute also to the CIA phenotypes. The *Eae39* C5 congenic fragment protected against CIA development, whereas the C19 and C20 subcongenic fragments enhanced CIA. Whether other genes downstream *Thrap2* have a protecting effect against arthritis awaits support from analogous experiments with that locus.

As mentioned in the introduction, *in vitro* experiments are key evidence of the relevance of a gene in a phenotype. Functional *in vitro* studies showed that *Thrap2* silencing elicited a decline of B cells specific death. Non-stimulated and LPS-stimulated splenic B cells in which *Thrap2* was inhibited had as a phenotype an increase in cell survival compared with the control cells ($P < 0.01$ and $P < 0.05$, respectively). Moreover, cell viability was markedly higher in *Thrap2* siRNA treated cells stimulated with LPS + anti-Ig and anti-CD40 than in control cells (Figure 4.10 A). A tendency to increase cell activation was also observed in cells where *Thrap2* was silenced (Figure 4.10 B). Interestingly, *Thrap2*-knockdown did not affect LN B cells viability (Figure 4.11). These findings suggest an organ-specific effect of Thrap2. Since Thrap2 is highly expressed on marginal zone in the spleen (see section 4.2.1), MZ B cells could be pinpointed as target cell-types. MZ B cells are involved in early immune response in adoptive immunity [110]. Indeed, CII-specific MZ B cells are found in naïve DBA1/J strain [111], which evidences that MZ B cells are key cells to the initial immune response to CII. On the other hand, MZ B cells are unique compared with other subpopulations, such as FO B cells in terms of activation status; MZ B cells respond more strongly than FO B cells and differentiate rapidly to plasmablast [110]. This brings about the possibility that *Thrap2*

may also play a role in FO B cells when they are fully activated. In that case, a longer activation period would be required to observe the effects of Thrap2 silencing *in vitro*.

Interestingly, transfection studies in CD4 T cell population demonstrated that *Thrap2* silencing does not affect cell survival or activation (Figure 4.12). Even though it was not possible to calculate specific cell death due to the lack of appropriate cell control (non-trasfected cells), the absence of influence of *Thrap2* in CD4 T cell *in vitro* culture was clearly shown.

LPS simulates T cell-independent response while anti-CD40 simulates T cell-dependent response. These data suggest that *Thrap2* affects B cell regardless of the activation mechanism, probably by survival signal. This hypothesis is supported by the putative common pathway between p53 and *Thrap2* identified by Ingenuity network analysis. This correlation is in turn supported by the reported control of Cdk8, subunit of the kinase module of the Mediator, over p53 target genes. Interestingly, p53 is a transcription factor known to be involved in B cell development and proliferation [112, 113]. It has been shown that p53 deficient mice resulted in an increase in pro-B cell [114] indicating a prominent role of p53 in apoptotic cell selection at an early stage in normal B cell development [114, 115]. On the other hand, Zelm et al. determined the upregulation of *Thrap2* in pro-B cell compared with other stages of B cell development [116]. These data was confirmed in the ImmGen Project which showed that pro-B cell have a higher expression of *Thrap2* than any other B cell subtype. Interestingly, *Thrap2* was upregulated in human common lymphoid progenitor (CLP) compared with multipotent stem cells, indicating a possible role of this gene in the developmental transition of multipotent stem cells to the CLP stage [117]. Meanwhile, *Thrap2* was not upregulated in T cell development [118] which could suggest a specific role of *Thrap2* in the B cell lineage. In summary, those findings indicate that *Thrap2* is actively involved in B cell development at different stages. In addition, they suggest that p53 and Thrap2 may interact and play a relevant role in pro-B cell development and selection.

Mutations or malfunctions of TF had already been associated with autoimmune disorders such as Stat4 in RA [30], p53 in RA [119], Foxp3 in IPEX [120] or T-bet in IBD and MS [121]. The results here presented imply that Thrap2 polymorphisms are

responsible for the strain-specific phenotypic differences. We hypothesize that DBA/1J variant alleles result in Thrap2 dysfunction *via* either a change in the three-dimensional structure or a decrease in the stability of *Thrap2* mRNA. The effect of loss of Thrap2 function might lead to enhanced B cells survival and activation, and consequently more severe autoimmune response. Presumably, to compensate this loss of protein activity, *Thrap2* expression is upregulated. This provides one explanation for the arthritic phenotype of mice carrying DBA/1J alleles in *Thrap2* and the increased expression of *Thrap2* in these mice. Clearly, these predictions warrant further studies to resolve how Thrap2 protein can control B cell survival/activation. A likely hypothesis is that Thrap2 regulates B cell survival through the p53 signaling pathway. Another likely hypothesis is that Thrap2 mediates transcription of Wnt/Wg target genes which play important roles in development. It has been shown that Med12 and Med13 are recruited for the transcription of Wingless (Wg) target genes [122]. Whether Thrap2 performs equivalent functions as its highly homologous Med13, or by contrast, each Mediator subunit specifically regulates transcription of distinct gene families, remains unknown. Finally, it is possible that Thrap2 regulates transcription of B cell survival factors and acts independently of p53 or Wnt/Wg pathways. Further elucidation of Thrap2 functions would help to understand how Thrap2 might operate in B cell survival, providing additional targets for the development of new autoimmunity therapies. Conditional deletion of Thrap2 in B cells is apparently necessary to address this decisive gap in our knowledge. For this purpose we are currently generating a B cell specific Thrap2 knockout mouse line. We have obtained from the NIH Knock-Out Mouse Project (KOMP) (www.komp.org) a Thrap2 knockout-first mouse line, Med13l$^{tm1a(KOMP)Wtsi}$, harboring a *Frt*-flanked βGeo cassette upstream of a *LoxP*-flanked exon 11 of Thrap2 gene. Thrap2 conditional allele are being created by crossing Med13l$^{tm1a(KOMP)Wtsi}$ mice to FLPe recombinase-expressing mice to remove the En2 splice acceptor and the βGeo cassette, and subsequently to B cell Cre recombinase-expressing mice to specifically delete exon 11 and inactivate Thrap2. Future *in vivo* studies will bring new insight into the function of Thrap2 and its role in autoimmunity.

In an effort to translate the result obtained in the CIA mouse model to the human, a candidate gene study was performed. It was showed that variations on the rs10507251 and rs9788041 SNPs, previously reported to be associated with RA in European and American with European ancestry cohorts, were not associated with susceptible to RA in our Egyptian cohort (Table 4.12). This is not surprising due to the already mentioned ethnic heterogeneity in genetic risk factors which characterizes RA. In fact, *PTPN22* and *PADI4* genes were not associated with RA in this Egyptian population, the largest RA Egyptian population studied to date (data not published). On the other hand, the SNP rs17580303, mapped in *MED13L*, was not a risk factor in this Egyptian cohort (Table 4.12). The rs17580303 SNP was chosen as a candidate SNP for this study due to its reported association with T1D in an American cohort with European ancestry. However, *MED13L* is a large gene (319,433 bp) containing 8,751 known genetic variations among which 4,432 are SNPs. In order to capture most of the variation, more than 100 Tag-SNPs would be necessary, according to Haploview software. Thus, to assess whether *MED13L* is linked to RA, further and deeper association shall be done including a high number of Tag-SNPs. In addition, 25 somatic mutations in human cancer mapping in *MED13L* have been reported (according to COSMIC). Whether any of those mutations may be a risk factor for RA is still to be explored.

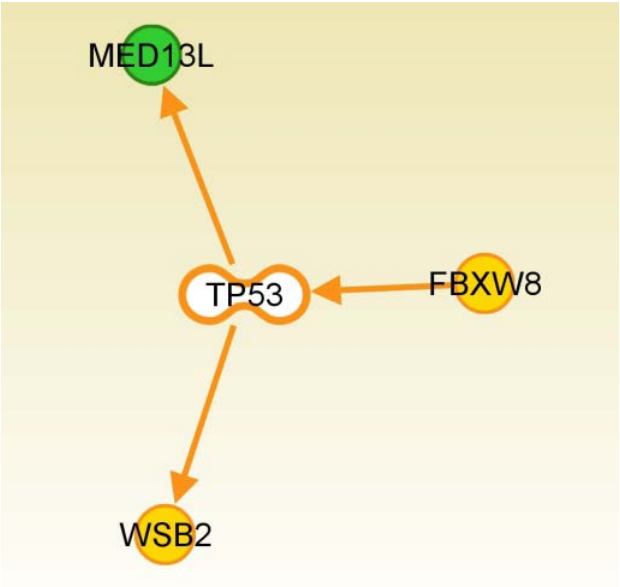

Figure 5.1. Interaction network between *Thrap2* and genes harbored in the C20 locus. Interaction identified by Ingenuity network analysis.

6 Conclusions

This work mapped loci implicated in arthritic clinical phenotypes in the BXD2/ TyJ model by using the power of mouse genetics. The most comprehensible genetic analysis on arthritis spontaneous model was performed with the identification of 21 QTLs associated with clinical phenotypes, 6 of which map in loci where no arthritic QTLs had been previously identified. In addition, the *Cia27* QTL was dissected into two loci. By integrating both genomic and functional data *Thrap2* was identified as gene that appears to impact CIA development and specific autoantibody production. Finally, *Thrap2* appeared to regulate B cells survival, and potentially, activation.

7 Summary

Rheumatoid arthritis (RA) is a systemic chronic autoimmune disorder characterized by inflammatory reactivity in the synovium of peripheral joints with unknown etiology. RA affects between 0.5-1% of the adult population and it is determined by both genetic and environmental factors. The HLA-DRB1 locus has the strongest contribution to RA, conferring around 50% of the overall genetic susceptibility. It has been challenging to identify further candidate genes contributing to RA pathogenesis due to the heterogeneity of the disease and the complex gene-gene and gene-environment interactions. Therefore, there is a compelling need to identify novel genetic factors governing RA in order to decipher the pathological mechanisms leading to disease. Having this background, the genetic determinants of two distinct mouse models, the spontaneous arthritis BXD2/TyJ strain and the collagen-induced arthritis (CIA) model, were studied in this thesis. In the first place, 366 mice of the fourth generation (G4) of a four-way autoimmune-prone advanced intercross line (AIL) were monitored for development of spontaneous arthritis. An arthritis incidence of 57.3% in females and 85.8% in males was observed. By an association study, 21 quantitative trait loci (QTLs) controlling susceptibility, maximum score and onset of disease were identified. In the second part of this work, the identification of the gene underlying the QTL *Cia27*, which was previously determined by our group, was addressed. Gene expression studies and congenic strain approaches were performed to fine map the QTL. *Thrap2* was identified to control clinical arthritis and autoantibody response. Subsequently, functional analysis of *Thrap2* indicated a role in B cell survival, suggesting an involvement of the gene in autoimmunity. Altogether, the present study shall provide new aid to solve the genetic etiology of RA and to gain a better understanding of the disease, which may eventually lead to the improvement of diagnostic methods and therapies.

7 Zusammenfassung

Die Rheumatoide Arthritis (RA) ist eine chronisch systemische Autoimmunerkrankung mit unbekannter Ätiologie, charakterisiert durch inflammatorische Prozesse im Synovium der peripheren Gelenke. Zwischen 0,5-1% der erwachsenen Bevölkerung ist von RA betroffen; einer Erkrankung, die sowohl genetisch als auch durch Umweltfaktoren determiniert ist. Der HLA-DRB1-Lokus hat den stärksten Einfluss auf die RA, mit einem Beitrag von ca. 50% der allgemeinen genetischen Suszeptibilität. Aufgrund der Heterogenität der Erkrankung sowie der komplexen Gen-Gen bzw. Gen-Umwelt-Wechselwirkungen, war es eine große Herausforderung weitere in die Pathogenese der RA involvierter Kandidatengene zu identifizieren. Daher ist es zwingend notwendig, neue genetische Faktoren für RA zu identifizieren, um die pathologischen Mechanismen, die zu dieser Erkrankung führen, zu entschlüsseln. Um dies zu erreichen, wurden im Rahmen dieser Doktorarbeit die genetischen Ursachen an zwei unabhängigen Mausmodellen, der spontanen Arthritis im BXD2/TyJ-Stamm sowie der Kollagen-induzierten Arthritis (CIA) untersucht. Im ersten Schritt wurde eine gemischte Zucht aus vier zu Autoimmunerkrankungen neigenden Inzuchtstämmen (four-way advanced intercross line, AIL) verwendet. Bei 366 Mäusen aus der vierten Generation (G4) dieser Zucht wurde untersucht, ob sich eine spontane Arthritis entwickelte. Das Auftreten einer Arthritis wurde bei 57,3% der Weibchen und bei 85,8% der Männchen beobachtet. Mit Hilfe einer Assoziationsstudie konnten 22 Genorte, sogenannte quantitative trait loci (QTLs), identifiziert werden, die Suszeptibilität die Ausprägung sowie den Beginn der Erkrankung kontrollieren. Im zweiten Schritt dieser Arbeit sollte das zu Grunde liegende Gen des QTLs *Cia27* identifiziert werden, welcher in früheren Arbeiten von unserer Gruppe identifiziert wurde. Dazu wurde der Chromosomenbereich des QTLs mit Hilfe von congenen Mauslinien sowie der Verwendung von Gen-Expressions-Daten weiter eingegrenzt und zwei eindeutige Loci identifiziert. *Thrap2*, welches das klinische Bild der Arthritis sowie die Autoantikörper-Antwort kontrolliert, wurde als das dem QTL *Cia27* zu Grunde liegende Gen identifiziert. Anschließend zeigten funktionelle Analysen, dass *Thrap2* eine wichtige Rolle für das Überleben von B-Zellen spielt, was darauf hindeutet, dass das Gen an Autoimmunprozessen beteiligt ist. Zusammengefasst leistet die vorliegende Studie einen Beitrag, die genetischen Ursachen und die Ätiologie der RA weiter

aufzuklären, um somit ein besseres Verständnis für die Erkrankung zu bekommen, welches schließlich zu einer verbesserten Diagnostik und Therapie führen kann.

8 References

1. Nishimura, K., et al., *Meta-analysis: diagnostic accuracy of anti-cyclic citrullinated peptide antibody and rheumatoid factor for rheumatoid arthritis.* Ann Intern Med, 2007. **146**(11): p. 797-808.
2. Nielen, M.M., et al., *Specific autoantibodies precede the symptoms of rheumatoid arthritis: a study of serial measurements in blood donors.* Arthritis Rheum, 2004. **50**(2): p. 380-6.
3. van der Helm-van Mil, A.H., et al., *Antibodies to citrullinated proteins and differences in clinical progression of rheumatoid arthritis.* Arthritis Res Ther, 2005. **7**(5): p. R949-58.
4. Aletaha, D., et al., *2010 Rheumatoid arthritis classification criteria: an American College of Rheumatology/European League Against Rheumatism collaborative initiative.* Arthritis Rheum, 2010. **62**(9): p. 2569-81.
5. Wienecke, T. and P.C. Gotzsche, *Paracetamol versus nonsteroidal anti-inflammatory drugs for rheumatoid arthritis.* Cochrane Database Syst Rev, 2004(1): p. CD003789.
6. Chen, Y.F., et al., *Cyclooxygenase-2 selective non-steroidal anti-inflammatory drugs (etodolac, meloxicam, celecoxib, rofecoxib, etoricoxib, valdecoxib and lumiracoxib) for osteoarthritis and rheumatoid arthritis: a systematic review and economic evaluation.* Health Technol Assess, 2008. **12**(11): p. 1-278, iii.
7. Donahue, K.E., et al., *Systematic review: comparative effectiveness and harms of disease-modifying medications for rheumatoid arthritis.* Ann Intern Med, 2008. **148**(2): p. 124-34.
8. Choy, E.H., et al., *A meta-analysis of the efficacy and toxicity of combining disease-modifying anti-rheumatic drugs in rheumatoid arthritis based on patient withdrawal.* Rheumatology (Oxford), 2005. **44**(11): p. 1414-21.
9. Kirwan, J.R., et al., *Effects of glucocorticoids on radiological progression in rheumatoid arthritis.* Cochrane Database Syst Rev, 2007(1): p. CD006356.
10. Ravindran, V., S. Rachapalli, and E.H. Choy, *Safety of medium- to long-term glucocorticoid therapy in rheumatoid arthritis: a meta-analysis.* Rheumatology (Oxford), 2009. **48**(7): p. 807-11.
11. Scott, D.L., *Biologics-based therapy for the treatment of rheumatoid arthritis.* Clin Pharmacol Ther, 2012. **91**(1): p. 30-43.
12. Helmick, C.G., et al., *Estimates of the prevalence of arthritis and other rheumatic conditions in the United States. Part I.* Arthritis Rheum, 2008. **58**(1): p. 15-25.
13. Symmons, D., et al., *The prevalence of rheumatoid arthritis in the United Kingdom: new estimates for a new century.* Rheumatology (Oxford), 2002. **41**(7): p. 793-800.
14. Carmona, L., et al., *Rheumatoid arthritis.* Best Pract Res Clin Rheumatol, 2010. **24**(6): p. 733-45.
15. Kalla, A.A. and M. Tikly, *Rheumatoid arthritis in the developing world.* Best Pract Res Clin Rheumatol, 2003. **17**(5): p. 863-75.
16. Pedersen, J.K., et al., *Incidence of rheumatoid arthritis from 1995 to 2001: impact of ascertainment from multiple sources.* Rheumatol Int, 2009. **29**(4): p. 411-5.
17. Carbonell, J., et al., *The incidence of rheumatoid arthritis in Spain: results from a nationwide primary care registry.* Rheumatology (Oxford), 2008. **47**(7): p. 1088-92.

18. Morgan, A.W., et al., *Reevaluation of the interaction between HLA-DRB1 shared epitope alleles, PTPN22, and smoking in determining susceptibility to autoantibody-positive and autoantibody-negative rheumatoid arthritis in a large UK Caucasian population.* Arthritis Rheum, 2009. **60**(9): p. 2565-76.
19. Liao, K.P., L. Alfredsson, and E.W. Karlson, *Environmental influences on risk for rheumatoid arthritis.* Curr Opin Rheumatol, 2009. **21**(3): p. 279-83.
20. Seldin, M.F., et al., *The genetics revolution and the assault on rheumatoid arthritis.* Arthritis Rheum, 1999. **42**(6): p. 1071-9.
21. MacGregor, A.J., et al., *Characterizing the quantitative genetic contribution to rheumatoid arthritis using data from twins.* Arthritis Rheum, 2000. **43**(1): p. 30-7.
22. Deighton, C.M., et al., *The contribution of HLA to rheumatoid arthritis.* Clin Genet, 1989. **36**(3): p. 178-82.
23. Stastny, P., *Association of the B-cell alloantigen DRw4 with rheumatoid arthritis.* N Engl J Med, 1978. **298**(16): p. 869-71.
24. Gregersen, P.K., J. Silver, and R.J. Winchester, *The shared epitope hypothesis. An approach to understanding the molecular genetics of susceptibility to rheumatoid arthritis.* Arthritis Rheum, 1987. **30**(11): p. 1205-13.
25. Lee, H.S., et al., *Several regions in the major histocompatibility complex confer risk for anti-CCP-antibody positive rheumatoid arthritis, independent of the DRB1 locus.* Mol Med, 2008. **14**(5-6): p. 293-300.
26. Begovich, A.B., et al., *A missense single-nucleotide polymorphism in a gene encoding a protein tyrosine phosphatase (PTPN22) is associated with rheumatoid arthritis.* Am J Hum Genet, 2004. **75**(2): p. 330-7.
27. Suzuki, A., et al., *Functional haplotypes of PADI4, encoding citrullinating enzyme peptidylarginine deiminase 4, are associated with rheumatoid arthritis.* Nat Genet, 2003. **34**(4): p. 395-402.
28. Plenge, R.M., et al., *TRAF1-C5 as a risk locus for rheumatoid arthritis--a genomewide study.* N Engl J Med, 2007. **357**(12): p. 1199-209.
29. Tsitsikov, E.N., et al., *TRAF1 is a negative regulator of TNF signaling. enhanced TNF signaling in TRAF1-deficient mice.* Immunity, 2001. **15**(4): p. 647-57.
30. Remmers, E.F., et al., *STAT4 and the risk of rheumatoid arthritis and systemic lupus erythematosus.* N Engl J Med, 2007. **357**(10): p. 977-86.
31. Kaplan, M.H., *STAT4: a critical regulator of inflammation in vivo.* Immunol Res, 2005. **31**(3): p. 231-42.
32. Kouskoff, V., et al., *Organ-specific disease provoked by systemic autoimmunity.* Cell, 1996. **87**(5): p. 811-22.
33. Keffer, J., et al., *Transgenic mice expressing human tumour necrosis factor: a predictive genetic model of arthritis.* EMBO J, 1991. **10**(13): p. 4025-31.
34. Taylor, B.A., et al., *Genotyping new BXD recombinant inbred mouse strains and comparison of BXD and consensus maps.* Mamm Genome, 1999. **10**(4): p. 335-48.
35. Stuart, J.M. and F.J. Dixon, *Serum transfer of collagen-induced arthritis in mice.* J Exp Med, 1983. **158**(2): p. 378-92.
36. Brackertz, D., G.F. Mitchell, and I.R. Mackay, *Antigen-induced arthritis in mice. I. Induction of arthritis in various strains of mice.* Arthritis Rheum, 1977. **20**(3): p. 841-50.
37. Courtenay, J.S., et al., *Immunisation against heterologous type II collagen induces arthritis in mice.* Nature, 1980. **283**(5748): p. 666-8.
38. Glant, T.T., et al., *Proteoglycan-induced arthritis in BALB/c mice. Clinical features and histopathology.* Arthritis Rheum, 1987. **30**(2): p. 201-12.

39. Schubert, D., et al., *Immunization with glucose-6-phosphate isomerase induces T cell-dependent peripheral polyarthritis in genetically unaltered mice.* J Immunol, 2004. **172**(7): p. 4503-9.
40. Mountz, J.D., et al., *Genetic segregation of spontaneous erosive arthritis and generalized autoimmune disease in the BXD2 recombinant inbred strain of mice.* Scand J Immunol, 2005. **61**(2): p. 128-38.
41. Corthay, A., et al., *Collagen-induced arthritis development requires alpha beta T cells but not gamma delta T cells: studies with T cell-deficient (TCR mutant) mice.* Int Immunol, 1999. **11**(7): p. 1065-73.
42. Svensson, L., et al., *B cell-deficient mice do not develop type II collagen-induced arthritis (CIA).* Clin Exp Immunol, 1998. **111**(3): p. 521-6.
43. Marques, A. and S. Muller, *Mouse models of autoimmune diseases.* Curr Drug Discov Technol, 2009. **6**(4): p. 262-9.
44. Holmdahl, R., et al., *High antibody response to autologous type II collagen is restricted to H-2q.* Immunogenetics, 1986. **24**(2): p. 84-9.
45. Wooley, P.H. and J.M. Chapedelaine, *Immunogenetics of collagen-induced arthritis.* Crit Rev Immunol, 1987. **8**(1): p. 1-22.
46. Peters, L.L., et al., *The mouse as a model for human biology: a resource guide for complex trait analysis.* Nat Rev Genet, 2007. **8**(1): p. 58-69.
47. Waterston, R.H., et al., *Initial sequencing and comparative analysis of the mouse genome.* Nature, 2002. **420**(6915): p. 520-62.
48. Abiola, O., et al., *The nature and identification of quantitative trait loci: a community's view.* Nat Rev Genet, 2003. **4**(11): p. 911-6.
49. Ahlqvist, E., M. Hultqvist, and R. Holmdahl, *The value of animal models in predicting genetic susceptibility to complex diseases such as rheumatoid arthritis.* Arthritis Res Ther, 2009. **11**(3): p. 226.
50. Flint, J., et al., *Strategies for mapping and cloning quantitative trait genes in rodents.* Nat Rev Genet, 2005. **6**(4): p. 271-86.
51. Jagodic, M., et al., *An advanced intercross line resolves Eae18 into two narrow quantitative trait loci syntenic to multiple sclerosis candidate loci.* J Immunol, 2004. **173**(2): p. 1366-73.
52. Darvasi, A. and M. Soller, *Advanced intercross lines, an experimental population for fine genetic mapping.* Genetics, 1995. **141**(3): p. 1199-207.
53. Yu, X., et al., *Using an advanced intercross line to identify quantitative trait loci controlling immune response during collagen-induced arthritis.* Genes Immun, 2007. **8**(4): p. 296-301.
54. Grupe, A., et al., *In silico mapping of complex disease-related traits in mice.* Science, 2001. **292**(5523): p. 1915-8.
55. Rogner, U.C. and P. Avner, *Congenic mice: cutting tools for complex immune disorders.* Nat Rev Immunol, 2003. **3**(3): p. 243-52.
56. Ibrahim, S.M. and X. Yu, *Dissecting the genetic basis of rheumatoid arthritis in mouse models.* Curr Pharm Des, 2006. **12**(29): p. 3753-9.
57. Wooley, P.H., et al., *Type II collagen-induced arthritis in mice. I. Major histocompatibility complex (I region) linkage and antibody correlates.* J Exp Med, 1981. **154**(3): p. 688-700.
58. Brunsberg, U., et al., *Expression of a transgenic class II Ab gene confers susceptibility to collagen-induced arthritis.* Eur J Immunol, 1994. **24**(7): p. 1698-702.
59. Bauer, K., et al., *Identification of new quantitative trait loci in mice with collagen-induced arthritis.* Arthritis Rheum, 2004. **50**(11): p. 3721-8.

60. Okroj, M., et al., *Rheumatoid arthritis and the complement system.* Ann Med, 2007. **39**(7): p. 517-30.
61. Sakaguchi, N., et al., *Altered thymic T-cell selection due to a mutation of the ZAP-70 gene causes autoimmune arthritis in mice.* Nature, 2003. **426**(6965): p. 454-60.
62. McIndoe, R.A., et al., *Localization of non-Mhc collagen-induced arthritis susceptibility loci in DBA/1j mice.* Proc Natl Acad Sci U S A, 1999. **96**(5): p. 2210-4.
63. Johansson, A.C., et al., *Genetic control of collagen-induced arthritis in a cross with NOD and C57BL/10 mice is dependent on gene regions encoding complement factor 5 and FcgammaRIIb and is not associated with loci controlling diabetes.* Eur J Immunol, 2001. **31**(6): p. 1847-56.
64. Lindvall, T., et al., *Dissection of a locus on mouse chromosome 5 reveals arthritis promoting and inhibitory genes.* Arthritis Res Ther, 2009. **11**(1): p. R10.
65. Otto, J.M., et al., *Identification of multiple loci linked to inflammation and autoantibody production by a genome scan of a murine model of rheumatoid arthritis.* Arthritis Rheum, 1999. **42**(12): p. 2524-31.
66. Glant, T.T., et al., *Disease-associated qualitative and quantitative trait loci in proteoglycan-induced arthritis and collagen-induced arthritis.* Am J Med Sci, 2004. **327**(4): p. 188-95.
67. Otto, J.M., et al., *A genome scan using a novel genetic cross identifies new susceptibility loci and traits in a mouse model of rheumatoid arthritis.* J Immunol, 2000. **165**(9): p. 5278-86.
68. Ji, H., et al., *Genetic influences on the end-stage effector phase of arthritis.* J Exp Med, 2001. **194**(3): p. 321-30.
69. Johnsen, A.K., et al., *Genome-wide and species-wide dissection of the genetics of arthritis severity in heterogeneous stock mice.* Arthritis Rheum, 2011. **63**(9): p. 2630-40.
70. Weis, J.J., et al., *Identification of quantitative trait loci governing arthritis severity and humoral responses in the murine model of Lyme disease.* J Immunol, 1999. **162**(2): p. 948-56.
71. Roper, R.J., et al., *Genetic control of susceptibility to experimental Lyme arthritis is polygenic and exhibits consistent linkage to multiple loci on chromosome 5 in four independent mouse crosses.* Genes Immun, 2001. **2**(7): p. 388-97.
72. Ma, Y., et al., *Interval-specific congenic lines reveal quantitative trait Loci with penetrant lyme arthritis phenotypes on chromosomes 5, 11, and 12.* Infect Immun, 2009. **77**(8): p. 3302-11.
73. Kamogawa, J., et al., *Arthritis in MRL/lpr mice is under the control of multiple gene loci with an allelic combination derived from the original inbred strains.* Arthritis Rheum, 2002. **46**(4): p. 1067-74.
74. Watson, W.C. and A.S. Townes, *Genetic susceptibility to murine collagen II autoimmune arthritis. Proposed relationship to the IgG2 autoantibody subclass response, complement C5, major histocompatibility complex (MHC) and non-MHC loci.* J Exp Med, 1985. **162**(6): p. 1878-91.
75. Brand, D.D., et al., *Autoantibodies to murine type II collagen in collagen-induced arthritis: a comparison of susceptible and nonsusceptible strains.* J Immunol, 1996. **157**(11): p. 5178-84.
76. Yu, X., et al., *Fine mapping of collagen-induced arthritis quantitative trait loci in an advanced intercross line.* J Immunol, 2006. **177**(10): p. 7042-9.
77. Livak, K.J. and T.D. Schmittgen, *Analysis of relative gene expression data using real-time quantitative PCR and the 2(-Delta Delta C(T)) Method.* Methods, 2001. **25**(4): p. 402-8.

78. Mougiakakos, D., et al., *Increased thioredoxin-1 production in human naturally occurring regulatory T cells confers enhanced tolerance to oxidative stress.* Blood, 2011. **117**(3): p. 857-61.
79. Asghari, F., et al., *Identification of quantitative trait loci for murine autoimmune pancreatitis.* J Med Genet, 2011. **48**(8): p. 557-62.
80. Plenge, R.M., et al., *Two independent alleles at 6q23 associated with risk of rheumatoid arthritis.* Nat Genet, 2007. **39**(12): p. 1477-82.
81. WTCCC, *Genome-wide association study of 14,000 cases of seven common diseases and 3,000 shared controls.* Nature, 2007. **447**(7145): p. 661-78.
82. Plomin, R., C.M. Haworth, and O.S. Davis, *Common disorders are quantitative traits.* Nat Rev Genet, 2009. **10**(12): p. 872-8.
83. Firestein, G.S., *Immunologic mechanisms in the pathogenesis of rheumatoid arthritis.* J Clin Rheumatol, 2005. **11**(3 Suppl): p. S39-44.
84. Stanich J., C.J., Whittum-Hudson J., Hudson A., *Rheumatoid arthritis: Disease or syndrome?* Open Access Rheumatology Research and Reviews, 2009. **1**: p. 179-192.
85. Weyand, C.M., P.A. Klimiuk, and J.J. Goronzy, *Heterogeneity of rheumatoid arthritis: from phenotypes to genotypes.* Springer Semin Immunopathol, 1998. **20**(1-2): p. 5-22.
86. Imboden, J.B., *The immunopathogenesis of rheumatoid arthritis.* Annu Rev Pathol, 2009. **4**: p. 417-34.
87. de Vries, R.R., et al., *Genetics of ACPA-positive rheumatoid arthritis: the beginning of the end?* Ann Rheum Dis, 2011. **70 Suppl 1**: p. i51-4.
88. McAllister K., E.S., Orozco G., *Genetics of rheumatoid arthritis: GWAS and beyond.* Open Access Rheumatology: Research and Reviews, 2011. **3**: p. 31–46.
89. Kochi, Y., et al., *Ethnogenetic heterogeneity of rheumatoid arthritis-implications for pathogenesis.* Nat Rev Rheumatol, 2010. **6**(5): p. 290-5.
90. Adarichev, V.A., et al., *Combined autoimmune models of arthritis reveal shared and independent qualitative (binary) and quantitative trait loci.* J Immunol, 2003. **170**(5): p. 2283-92.
91. Blankenhorn, E.P., et al., *Genetic analysis of the influence of pertussis toxin on experimental allergic encephalomyelitis susceptibility: an environmental agent can override genetic checkpoints.* J Immunol, 2000. **164**(6): p. 3420-5.
92. Kono, D.H., et al., *Lupus susceptibility loci in New Zealand mice.* Proc Natl Acad Sci U S A, 1994. **91**(21): p. 10168-72.
93. Vegvari, A., et al., *Two major interacting chromosome loci control disease susceptibility in murine model of spondyloarthropathy.* J Immunol, 2005. **175**(4): p. 2475-83.
94. Merriman, T.R., et al., *Suggestive evidence for association of human chromosome 18q12-q21 and its orthologue on rat and mouse chromosome 18 with several autoimmune diseases.* Diabetes, 2001. **50**(1): p. 184-94.
95. Raychaudhuri, S., et al., *Genetic variants at CD28, PRDM1 and CD2/CD58 are associated with rheumatoid arthritis risk.* Nat Genet, 2009. **41**(12): p. 1313-8.
96. Ueda, H., et al., *Association of the T-cell regulatory gene CTLA4 with susceptibility to autoimmune disease.* Nature, 2003. **423**(6939): p. 506-11.
97. Korstanje, R. and B. Paigen, *From QTL to gene: the harvest begins.* Nat Genet, 2002. **31**(3): p. 235-6.
98. Gay, S., R.E. Gay, and W.J. Koopman, *Molecular and cellular mechanisms of joint destruction in rheumatoid arthritis: two cellular mechanisms explain joint destruction?* Ann Rheum Dis, 1993. **52 Suppl 1**: p. S39-47.
99. Meinecke, I., et al., *The role of synovial fibroblasts in mediating joint destruction in rheumatoid arthritis.* Curr Pharm Des, 2005. **11**(5): p. 563-8.

100. Mebius, R.E. and G. Kraal, *Structure and function of the spleen.* Nat Rev Immunol, 2005. **5**(8): p. 606-16.
101. Karlsson, J., et al., *Novel quantitative trait loci controlling development of experimental autoimmune encephalomyelitis and proportion of lymphocyte subpopulations.* J Immunol, 2003. **170**(2): p. 1019-26.
102. Morel, L., et al., *The major murine systemic lupus erythematosus susceptibility locus, Sle1, is a cluster of functionally related genes.* Proc Natl Acad Sci U S A, 2001. **98**(4): p. 1787-92.
103. Ahlqvist, E., R. Bockermann, and R. Holmdahl, *Fragmentation of two quantitative trait loci controlling collagen-induced arthritis reveals a new set of interacting subloci.* J Immunol, 2007. **178**(5): p. 3084-90.
104. Muncke, N., et al., *Missense mutations and gene interruption in PROSIT240, a novel TRAP240-like gene, in patients with congenital heart defect (transposition of the great arteries).* Circulation, 2003. **108**(23): p. 2843-50.
105. Musante, L., et al., *cDNA cloning and characterization of the human THRAP2 gene which maps to chromosome 12q24, and its mouse ortholog Thrap2.* Gene, 2004. **332**: p. 119-27.
106. Sato, S., et al., *A set of consensus mammalian mediator subunits identified by multidimensional protein identification technology.* Mol Cell, 2004. **14**(5): p. 685-91.
107. Conaway, R.C. and J.W. Conaway, *Function and regulation of the Mediator complex.* Curr Opin Genet Dev, 2011. **21**(2): p. 225-30.
108. Conaway, R.C., et al., *The mammalian Mediator complex and its role in transcriptional regulation.* Trends Biochem Sci, 2005. **30**(5): p. 250-5.
109. Daoud, S.S., et al., *Impact of p53 knockout and topotecan treatment on gene expression profiles in human colon carcinoma cells: a pharmacogenomic study.* Cancer Res, 2003. **63**(11): p. 2782-93.
110. Pillai, S., A. Cariappa, and S.T. Moran, *Marginal zone B cells.* Annu Rev Immunol, 2005. **23**: p. 161-96.
111. Carnrot, C., et al., *Marginal zone B cells are naturally reactive to collagen type II and are involved in the initiation of the immune response in collagen-induced arthritis.* Cell Mol Immunol, 2011. **8**(4): p. 296-304.
112. Schmidt, N.W., et al., *p53 regulates Btk-dependent B cell proliferation but not differentiation.* J Leukoc Biol, 2006. **79**(4): p. 852-9.
113. Phan, R.T. and R. Dalla-Favera, *The BCL6 proto-oncogene suppresses p53 expression in germinal-centre B cells.* Nature, 2004. **432**(7017): p. 635-9.
114. Lu, L., D. Lejtenyi, and D.G. Osmond, *Regulation of cell survival during B lymphopoiesis: suppressed apoptosis of pro-B cells in P53-deficient mouse bone marrow.* Eur J Immunol, 1999. **29**(8): p. 2484-90.
115. Slatter, T.L., et al., *p53-mediated apoptosis prevents the accumulation of progenitor B cells and B-cell tumors.* Cell Death Differ, 2010. **17**(3): p. 540-50.
116. van Zelm, M.C., et al., *Ig gene rearrangement steps are initiated in early human precursor B cell subsets and correlate with specific transcription factor expression.* J Immunol, 2005. **175**(9): p. 5912-22.
117. Hoebeke, I., et al., *T-, B- and NK-lymphoid, but not myeloid cells arise from human CD34(+)CD38(-)CD7(+) common lymphoid progenitors expressing lymphoid-specific genes.* Leukemia, 2007. **21**(2): p. 311-9.
118. Dik, W.A., et al., *New insights on human T cell development by quantitative T cell receptor gene rearrangement studies and gene expression profiling.* J Exp Med, 2005. **201**(11): p. 1715-23.

119. Yamanishi, Y., et al., *Regional analysis of p53 mutations in rheumatoid arthritis synovium.* Proc Natl Acad Sci U S A, 2002. **99**(15): p. 10025-30.
120. van der Vliet, H.J. and E.E. Nieuwenhuis, *IPEX as a result of mutations in FOXP3.* Clin Dev Immunol, 2007. **2007**: p. 89017.
121. Peng, S.L., *The T-box transcription factor T-bet in immunity and autoimmunity.* Cell Mol Immunol, 2006. **3**(2): p. 87-95.
122. Carrera, I., et al., *Pygopus activates Wingless target gene transcription through the mediator complex subunits Med12 and Med13.* Proc Natl Acad Sci U S A, 2008. **105**(18): p. 6644-9.

9 Appendix

9.1 Abbreviations

7-AAD	7-Amino-Actinomycin D
ACPA	autoantibodies to citrullinated protein antigens
ACR	American College of Rheumatology
AIL	advanced intercross line
AP	alkaline phosphatase
APC	allophycocyanin
AUC	area under the curve
B10q	B10.D1-H2q/SgJ: C57BL/10 strain with H2q haplotype of MHC
bp	base pair
BSA	bovine serum albumin
CII	type II collagen
CVII	type VII collagen
cDNA	complementary DNA
CFA	complete Freund's adjuvant
Chr	chromosome
CIA	collagen-induced arthritis
CLP	common lymphoid progenitor
DAPI	4’,6-diamidino-2-phenylindole
DC	dendritic cell
DMARD	disease modifying antirheumatic drug
DNA	deoxyribonucleic acid
EAE	experimental autoimmune encephalomyelitis
EDTA	ethylenediaminetetraacetic acid
ELISA	enzyme-linked immunosorbent assay

EULAR	European League Against Rheumatism
Exo	Exonuclease I
F2	F2 intercross
FACS	fluorescence activated cell sorting (used as flow cytometry synonym)
FCS	fetal calf serum
FITC	fluorescein isothiocyanate
FO	follicular
G4	fourth generation
GWAS	genome-wide association study
h	hour
HKG	housekeeping gene
HRP	horseradish peroxidase
IBD	inflammatory bowel disease
IFA	incomplete Freund's adjuvant
Ig	immunoglobulin
IP	interrogation primer
LN	lymph nodes
LOD	logarithm of the odds
LPS	lipopolysaccharide
M	molar
mAb	monoclonal antibody
MACS	magnetic cell sorting
MA	minor allele
MAF	minor allele frequency
Mbp	mega base pairs
mg	milligram
MHC	major histocompatibility complex
min	minute
ml	milliliter

MS	multiple sclerosis
MZ	marginal zone
n	number
N2	N2 backcross
OD	optical density
OR	odd ratio
OVA	ovalbumin
P	*P* value
PALS	periarteriolar lymphatic sheath
PBS	phosphate buffered saline
PCR	polymerase chain reaction
PE	phycoerythrin
PerCp	peridinin chlorphyll protein
PGIA	proteoglycan induced arthritis
QT	quantitative trait
QTL	quantitative trait locus
RA	rheumatoid arthritis
RF	rheumatoid factor
RNA	ribonucleic acid
RNAPII	RNA polymerase II
RP	red pulp
RT	room temperature
s	second
SAP	Shrimp Alkaline Phosphatase
SD	standard deviation
SEM	standard error of the mean
RFLP	restriction fragment length polymorphism
siRNA	small interfering RNA
SLE	systemic lupus erythematosus
SLS	Sample Loading Solution

SNP	single nucleotide polymorphism
SP	spleen
T1D	type 1 diabetes
TAE	tris-acetate-EDTA buffer
TF	transcription factor
µg	microgram
µl	microlitre
wg	wingless

9.2 List of figures

9.3 List of tables

10 Acknowledgements

I would like to acknowledge all the people who have supported me during these years of work. Unfortunately, I cannot mention all of them, nevertheless, I assure them all of my sincerest thanks.

First of all, I would like to express my immense gratitude to my supervisor Prof. Saleh Ibrahim, for giving me the opportunity to work in his group and for guiding me through these years. His constructive criticism, great support and optimism towards my work have motivated me at every stage of this thesis.

I would like to show my sincerest appreciation to Prof. Detlef Zillikens, director of the Department of Dermatology, for hosting this thesis.

I am very grateful to Prof. Rudolf Manz for all the great support in the *in vitro* experiment, the valuable suggestions and constructive comments on this thesis. I would also like to thank the members of his group for their support.

I would like to thank Prof Rikard Holmdahl for kindly providing the subcongenic strains.

Kathrin Kalies I thank for the collaboration in the microdissection study.

I am indebted to all the past and present members from the Department of Dermatology who contributed in any way to my work and supported me during these years. Particularly, I would like to thank Dr. Steffen Möller for the invaluable bioinformatic support, for his HAPPY being and the good chats. Andreia de Castro I have to thank for teaching me all I had to know about *Cia27* and mouse genetics when I first started in the lab, for her practical support. I would like to thank Dr. Misa Hirose for her good advices in any matter, for the company during these years and the very helpful corrections on the manuscript. Special thanks go to Miriam Freitag for the excellent technical assistance and lab organization which allows things to run as they should run. I would like also to thank Dr. Andreas Recke for his advice in statistics and his attitude always to help. Yask Gupta and Girish Srinivas I would like to thank for the bioinformatic

support and the good moments in the lab. Thanks goes to Miriam Daumann for taking care of the mice.

These years would have been very different if I had not had the enormous luck to meet Katerina Vafia. I would like to thank her for her unconditional support and for the many great moments together.

I also would like to thank my friends for the moral support and for cheering me always up. Especially, I would like to thank my old team, Danielle, Alberto and Miguel, who are the ones I started my scientific life with and from whom I learned much more than science. They have been during these years support and example.

I am really thankful to my sister and my parents for being there for me in every conceivable way. Thanks for the many visits that made the distance shorter.

And a special thanks to Frank, for his encouragement and patience. Thanks for spending all these years next to me.

11 *Curriculum vitae*